Stockholm University

Using Lyα to illuminate the circumgalactic medium and the Epoch of Reionization

Lessons from low redshift

Axel Runnholm

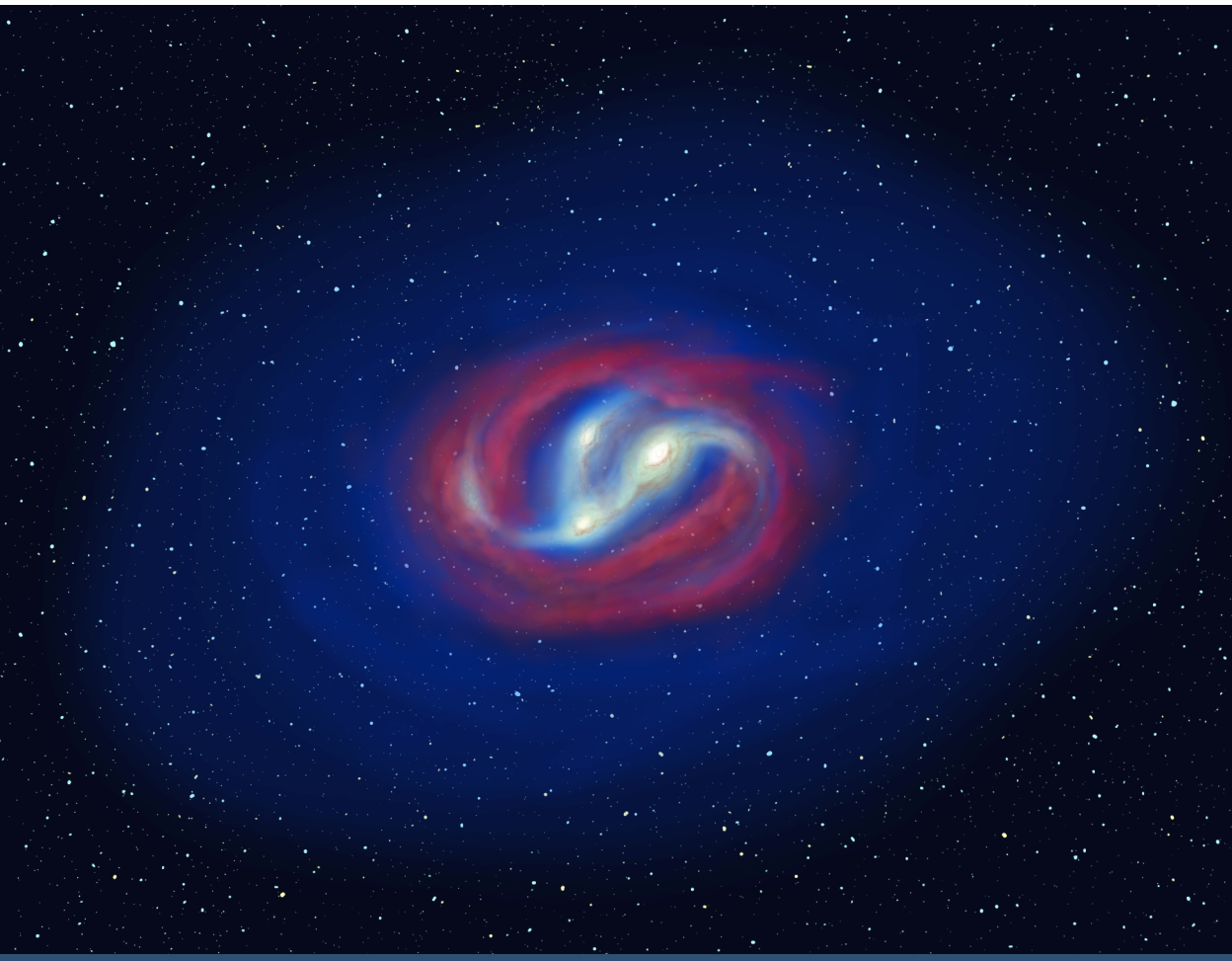

Doctoral Thesis in Astronomy at Stockholm University, Sweden 2022

Using Lyα to illuminate the circumgalactic medium and the Epoch of Reionization

Lessons from low redshift

Axel Runnholm

Academic dissertation for the Degree of Doctor of Philosophy in Astronomy at Stockholm University to be publicly defended on Wednesday 14 September 2022 at 13.00 in The Svedberg-salen (FD5), AlbaNova universitetscentrum, Roslagstullsbacken 21 and online via Zoom, public link is available at the department website.

Abstract

The field of extragalactic astronomy is progressing rapidly but there is still much to understand and many questions that remain open. During recent years the Lyα emission line has come to the fore as a potentially very powerful astrophysical tool and is now routinely used to find galaxies at the very highest redshifts. However, using Lyα is complicated by the fact that it is a resonant line, which means that it undergoes radiative transfer as it travels through neutral hydrogen when escaping from galaxies. This makes Lyα observations very difficult to interpret, but it also means that Lyα can provide information about the neutral hydrogen in the universe, giving it the potential to, for instance, map the progression of the Epoch of Reionization—the large scale phase transition during which the universe went from being completely neutral to being dominated by ionized gas.

In order to make the most of Lyα observations and extend its usefulness even further we need to understand exactly what kind of galaxies emit Lyα, and, by extension, which physical processes control its escape. Even though Lyα is relatively easy to detect at high redshift we cannot study the details of the escape process there, due to the lack of additional information about the emitting galaxies. In order to understand Lyα in detail then, we need to observe galaxies at much lower redshift where we can get more information. This is the main driver of the projects included in this thesis which focuses on furthering our understanding of Lyα using local universe observations.

We find that Lyα escape is a strongly multivariate issue and that using simple machine learning techniques can both help us predict Lyα and determine what the main drivers of Lyα emission are. We present two studies focusing on multivariate prediction of both imaging and spectral observations of Lyα showing that it is, in general, possible to predict the total Lyα luminosity very well but that the equivalent width and the escape fraction still remain somewhat elusive. We show that the primary variables controlling of Lyα seem to be the production rate of Lyα photons and the ionization state of the surrounding gas.

We also study the spatial distribution of extended Lyα halo emission in an effort to determine how important spatial scattering of Lyα is and whether the properties of halos change between low and high redshift. We find that halos at low redshift are remarkably consistent with high redshift results but that the extended emission most likely is not solely due to scattering of Lyα photons produced in the central galaxy but is also produced by faint stellar components at large radii, something not demonstrated before.

Lastly, we present a database of Lyα spectral profiles and use that dataset to examine the evolution of Lyα spectra as a function of redshift. The profiles show clear trends, with blueshifted emission becoming markedly less prominent at high redshifts. Using a prescription for the expected attenuation of the intergalactic medium, we show that the evolution in the profiles is consistent with the intrinsic line shape not evolving between redshift 0 and redshift 6. We also present work analyzing correlations of Lyα with both stellar population and nebular gas properties in extensive detail shedding further light on what properties makes a galaxy a Lyα emitter.

Keywords: *Lyman alpha galaxies, Starburst galaxies, Galaxy evolution, Epoch of Reionization, Circumgalactic medium.*

Stockholm 2022
http://urn.kb.se/resolve?urn=urn:nbn:se:su:diva-207633

ISBN 978-91-7911-954-6
ISBN 978-91-7911-955-3

Stockholm University

Department of Astronomy

Stockholm University, 106 91 Stockholm

USING LYA TO ILLUMINATE THE CIRCUMGALACTIC MEDIUM AND THE EPOCH OF REIONIZATION

Axel Runnholm

Stockholm
University

Using Lyα to illuminate the circumgalactic medium and the Epoch of Reionization

Lessons from low redshift

Axel Runnholm

ISBN print 978-91-7911-954-6
ISBN PDF 978-91-7911-955-3

Printed in Sweden by Universitetsservice US-AB, Stockholm 2022

Abstract

The field of extragalactic astronomy is progressing rapidly but there is still much to understand and many questions that remain open. During recent years the Lyα emission line has come to the fore as a potentially very powerful astrophysical tool and is now routinely used to find galaxies at the very highest redshifts. However, using Lyα is complicated by the fact that it is a resonant line, which means that it undergoes radiative transfer as it travels through neutral hydrogen when escaping from galaxies. This makes Lyα observations very difficult to interpret, but it also means that Lyα can provide information about the neutral hydrogen in the universe, giving it the potential to, for instance, map the progression of the Epoch of Reionization—the large scale phase transition during which the universe went from being completely neutral to being dominated by ionized gas.

In order to make the most of Lyα observations and extend its usefulness even further we need to understand exactly what kind of galaxies emit Lyα and, by extension, which physical processes control its escape. Even though Lyα is relatively easy to detect at high redshift we cannot study the details of the escape process there, due to the lack of additional information about the emitting galaxies. In order to understand Lyα in detail then, we need to observe galaxies at much lower redshift where we can get more information. This is the main driver of the projects included in this thesis which focuses on furthering our understanding of Lyα using local universe observations.

We find that Lyα escape is a strongly multivariate issue and that using simple machine learning techniques can both help us predict Lyα and determine what the main drivers of Lyα emission are. We present two studies focusing on multivariate prediction of both imaging and spectral observations of Lyα showing that it is, in general, possible to predict the total Lyα luminosity very well but that the equivalent width and the escape fraction still remain somewhat elusive. We show that the primary variables controlling of Lyα seem to be the

production rate of Lyα photons and the ionization state of the surrounding gas.

We also study the spatial distribution of extended Lyα halo emission in an effort to determine how important spatial scattering of Lyα is and whether the properties of halos change between low and high redshift. We find that halos at low redshift are remarkably consistent with high redshift results but that the extended emission most likely is not solely due to scattering of Lyα photons produced in the central galaxy but is also produced by faint stellar components at large radii, something not demonstrated before.

Lastly, we present a database of Lyα spectral profiles and use that dataset to examine the evolution of Lyα spectra as a function of redshift. The profiles show clear trends, with blueshifted emission becoming markedly less prominent at high redshifts. Using a prescription for the expected attenuation of the intergalactic medium, we show that the evolution in the profiles is consistent with the intrinsic line shape not evolving between redshift 0 and redshift 6. We also present work analyzing correlations of Lyα with both stellar population and nebular gas properties in extensive detail shedding further light on what properties makes a galaxy a Lyα emitter.

Sammanfattning

Forskningsfältet extragalaktisk astronomi gör enorma framsteg men det finns fortfarande mycket vi inte förstår och många öppna frågor. Ett exempel är den storskaliga fasövergången som kallas Återjoniseringsepoken då vårt universum gick från att vara helt neutralt till att domineras av joniserad gas. Hur gick övergången till och vilka var källorna till den joniserande strålningen?

Under senare år har Lyman α (Lyα) emissionslinjen dykt upp som ett potentiellt kraftfullt astrofysiskt verktyg. Den används nu till exempel rutinmässigt för att upptäcka galaxer vid de högsta observerade rödförskjutningarna. Att använda Lyα kompliceras dock av att det är en resonant linje, vilket innebär att den genomgår strålningstransport när den färdas genom neutralt väte på väg ut ur galaxer. Detta gör Lyα-observationer mycket komplexa att tolka, men det betyder också att de är potentiellt användbara för att få information om det neutrala vätet i universum. Detta betyder att de till exempel skulle kunna användas för att kartlägga Återjoniseringsepoken.

För att effektivt kunna använda Lyα-observationer och potentiellt utvidga dess användningsområden behöver vi förstå vilka typer av galaxer det är som utsänder Lyα och därmed vilka fysiska processer som kontrollerar dess utsändning. Även om Lyα-utsändande galaxer är relativt lätta att detektera vid hög rödförskjutning så kan vi inte studera detaljerna i deras utsändningsprocesser på grund av bristen på oberoende information om galaxerna. För att förstå detaljerna så behöver vi observera galaxer vid mycket lägre rödförskjutningar där vi kan få mer information. Detta är den huvudsakliga drivkraften för den här avhandlingen som fokuserar på hur vi kan använda observationer av närliggande galaxer för att bättre förstå Lyα.

Vi visar att Lyα-flykt från galaxer är ett starkt multivariat problem, och att enkla maskininlärningstekniker kan hjälpa oss att förutsäga galaxers Lyα-strålning, både observerad som bilder och som spektra, och utröna de huvudsakliga drivkrafterna bakom Lyα-strålning. Vi presenterar två studier som fo-

kuserar på multivariatförutsägelser av Lyα och visar att det generellt sett är möjligt att förutsäga Lyα till hög noggrannhet men att ekvivalentbredden och andelen av Lyα fotoner som tar sig ut ur systemet ($f_{esc}^{Ly\alpha}$) fortfarande är svårförutsagda. Vi visar också att de primära variablerna som kontrollerar Lyα verkar vara produktionstakten av Lyα-fotoner och joniseringsgraden hos den kringliggande gasen.

Vi studerar även fördelningen av utsträckt Lyα-emission runt galaxer i ett försök att komma fram till hur viktig spatial omfördelning av Lyα är och huruvida galaxhaloegenskaper ändras mellan låg och hög rödförskjutning. Det vi ser är att Lyα-halos är förvånansvärt lika mellan hög och låg rödförskjutning och även att de förmodligen inte produceras endast av omfördelningsprocesser utan även av en utsträckt ljussvag stjärnpopulation, vilket inte setts tidigare.

Till sist presenterar vi en publik databas av Lyα-spektralprofiler och använder det datasetet för att undersöka utvecklingen av Lyα-spektra som en funktion av rödförskjutning. Profilerna visar tydliga trender, t.ex. att emission på den blå sidan av linjen blir mindre tydlig vid hög rödförskjutning. Genom att använda ett uppmätt medelvärde av absorption från det intergalaktiska mediet visar vi att profilerna är helt konsekventa med att profilen som kommer ut ur galaxerna är oförändrad mellan rödförskjutning 0 och 6.

List of papers

The following papers, referred to in the text by their Roman numerals, are included in this thesis.

Paper I. **Runnholm, A.**, Hayes, M., Melinder, J., Rivera-Thorsen, E., Östlin, G., Cannon, J., Kunth, D.: The Lyman Alpha Reference Sample. X. Predicting Lya Output from Star-forming Galaxies Using Multivariate Regression, *The Astrophysical Journal*, 892, 48 (2020), doi:10.3847/1538-4357/ab7a91

Paper II. **Runnholm, A.**, Hayes, M., Lin, Y., Melinder, J., Scarlata,C., Adamo, A., Bik, A., Blaizot, J., Cannon, J., Cantalupo, S., Garel, T., Gronke, M., Herenz, E., Leclercq, F., Östlin, G., Peroux, C., Rasekh, A., Rutkowski, M., Verhamme, A., Wisotzki, L. : On the evolution of the size of Lyman alpha halos across cosmic time: no change in the circumgalactic gas distribution when probed by line emission, *(Submitted to MNRAS)*

Paper III. **Runnholm, A.**, Gronke, M., Hayes, M.: The Lyman Alpha Spectral Database (LASD), *PASP*, 133, 1021, (2021), doi:10.1088/1538-3873/abe3ca

Paper IV. Hayes, M., **Runnholm, A.**, Gronke, M., Scarlata, C.: Spectral Shapes of the Ly Emission from Galaxies. I. Blueshifted Emission and Intrinsic Invariance with Redshift. *The Astrophysical Journal*, 908, 1, id.36, 17 pp (2021). doi:10.3847/1538-4357/abd246

Paper V. Hayes, M., **Runnholm, A.**, Scarlata, C., Gronke, M., T. Emil Rivera-Thorsen: Spectral Shapes of the Ly Emission from Galaxies. II. the influence of stellar properties and nebular conditions on the emergent line profiles (draft manuscript)

Papers not included in this thesis

- Adamo, A., Hollyhead, K., Messa, M., Ryon, J. E., Bajaj, V., **Runnholm, A.**, Aalto, S., Calzetti, D., Gallagher, J. S., Hayes, M. J., Kruijssen, J. M. D., König, S., Larsen, S. S., Melinder, J., Sabbi, E., Smith, L. J., Östlin, G., Star cluster formation in the most extreme environments: insights from the HiPEEC survey, *Monthly Notices of the Royal Astronomical Society*, 499, 3, (2020)

- Östlin, G., Rivera-Thorsen, T. E., Menacho, V., Hayes, M., **Runnholm, A.**, Micheva, G., Oey, M. S., Adamo, A., Bik, A., Cannon, J., Gronke, M., Kunth, D., Laursen, P., Mas-Hesse, J. M., Melinder, J., Messa, M., Sirressi, M., Smith, L., The Source of Leaking Ionizing Photons from Haro11: Clues from HST/COS Spectroscopy of Knots A, B, and C, *The Astrophysical Journal* 912, 2, id.155, (2021)

- Sirressi, M., Adamo, A., Hayes, M., Bik, A., Strandänger, M., **Runnholm, A.**, Oey, M. S., Östlin, G., Menacho, V., Smith, L. J., Haro 11 - Untying the knots of the nuclear starburst, *Monthly Notices of the Royal Astronomical Society*, 510, 4, pp.4819-4836 (2022)

- Rasekh, A., Melinder, J., Östlin, G., Hayes, M., Herenz, E. C., **Runnholm, A.**, Kunth, D., Mas Hesse, J. M., Verhamme, A., Cannon, J. M., The Lyman Alpha Reference Sample. XII. Morphology of extended Lyman alpha emission in star-forming galaxies, Astronomy & Astrophysics, 662, id.A64, 62 pp. (2022)

Author's contribution

Paper I. The data used in this paper have been obtained as a part of the Lyman Alpha Reference Sample project and have been reduced and measured by many members of that team. I was responsible for collating the data as well as making new measurements, primarily of the optical emission lines and the UV sizes of the galaxies. I performed all of the data-analysis in the paper, developed codes for normalizing data sets, fitting our multivariate relations, and determining variable importance. Additionally I interpreted the results and wrote the large majority of the manuscript.

Paper II. I developed the technical database management code and the web interface. I also took part in the development of the online analysis codes and led the algorithm testing and optimization efforts. I wrote approximately half of the manuscript.

Paper III. I performed the majority of the data processing from raw HST data to finished data product. The only analysis steps for which I was not the main contributor was dark current subtraction, and PSF matching. Additionally I did all of the data analysis and wrote the majority of the manuscript with input from co-authors.

Paper IV. The paper is heavily based on the work from **Paper II** where I designed and implemented the algorithms to make the fundamental measurements of Lyα profile shapes which we used in this paper. My main contribution was an extensive evaluation of the redshift detection algorithm in the LASD and a calibration of the effects of spectral resolution on the redshift measurements enabling the stacking analysis used in this pa-

per. I also collaborated and commented on the manuscript.

Paper V. This paper is also based on the work from **Paper II** and relies on the methods we developed there for all Lyα spectral measurements. My primary additional contribution was section 8 about the multivariate analysis and prediction. For this I developed the code and did the analysis as well as wrote the text for the section. I also gave comments on the manuscript as a whole.

Reused and new material

This thesis partly uses the material presented in my licentiate thesis which contained Papers I and II. The material has in most cases been substantially reworked but the main text sources are:

Chapter 1 consists exclusively of new material.

Chapter 2 consists exclusively of new material.

Chapter 3 primarily consists of material adapted from Chapter 2 of the Licentiate.

Chapter 4 has been adapted from content from Chapter 4.3 and 4.4 of the Licentiate

Chapter 5 has a combination of new and reworked material. Chapter 5.1 has some material from Chapter 3.1.1 of the licentiate but the majority of the discussion is new material, in particular the discussion of Lyα halos. The discussion of LARS is adapted from Chapter 5.2 of the licentiate but has new material related to the spatial extension of the LARS galaxies. Chapter 5.2.2 and 5.2.3 are all new material.

Chapter 6 again a combination of new and reused material. In particular Chapter 6.1 adapted from Chapter 4.1 of the licentiate, and Chapter 6.2 and 6.3 are combinations of new material and reworked text from licentiate Chapter 4.3.2.

Chapter 7 consists exclusively of new material.

Contents

Abbreviations

ACS	Advanced Camera for Surveys
CGM	Circumgalactic Medium
CMB	Cosmic Microwave Background
eLARS	extended Lyman Alpha Reference Sample
EoR	Epoch of Reionization
EW	Equivalent Width
$\mathbf{f}_{\mathrm{esc}}^{\mathrm{Ly}\alpha}$	Escape Fraction of Lyα
FUV	Far Ultraviolet
GALEX	Galaxy Evolution Explorer
HST	Hubble Space Telescope
IGM	Intergalactic Medium
IR	Infrared
ISM	Interstellar medium
JWST	James Webb Space Telescope
LAE	Lyman α Emitter
LARS	Lyman Alpha Reference Sample
LBG	Lyman Break Galaxy
LIS	Low Ionization State
Lyα	Lyman α
LyC	Lyman Continuum. Hydrogen ionizing radiation
SB	Surface Brightness
SBC	Solar Blind Channel
SDSS	Sloan Digital Sky Survey

SED Spectral Energy Distribution

SFR Star-formation Rate

SKA Square Kilometer Array

1. The popular science introduction: The bigger context

This short introductory chapter is here to set the scene and serve as a quick introduction to astronomy in general and extragalactic astronomy in particular for the general public. If you are part of the astronomical research community you should probably skip ahead to Chapter 2.

When studying extragalactic astronomy we are concerned with some of the largest scale questions it is possible to study—such as "What did the universe look like when it just formed?", "How did our galaxy form?", "What will happen to it in the future?". It is therefore quite fair to say that when we say we want to look at "the big picture" it is pretty much the biggest picture one can look at. So let's go!

Right after the creation of the universe in the Big Bang, matter is very hot. This is quite understandable, and I'd like to believe that you or I would also be feeling somewhat hot and bothered if someone squeezed us into an infinitesimally small space. In fact, the universe at this time is hot enough to fuse protons together—forming new elements such as helium and lithium. However, during this epoch the universe is getting bigger very rapidly. As the volume increases, the temperature drops and the free floating protons and electrons of the early universe soup start to bond together and matter gradually becomes dominated by neutral hydrogen gas.

The following period of time is often referred to as the Dark Ages as there are not yet any stars to light up the darkness. This does not last long however, as gravity starts doing its magic and matter, both dark and otherwise, clumps together and forms the first stars (unintuitively named Population III stars) and galaxies. The intense radiation coming from the newborn stars heat the gas around them, and the protons and electrons that just stuck together get pried

apart again, gradually bringing the universe back to an ionized state. The re-ionization process, most often referred to as the Epoch of Reionization (EoR), takes quite a long time and, during this period, galaxies develop further and the rate of star formation of the universe increases. Around 12.5 billion years ago, the universe is (probably) fully ionized and then enters the period known as Cosmic Noon when star-formation is at its height. This period of furious activity peaks at around 10 billion years ago when the universe was forming stars at 8 times the rate we see today (Madau and Dickinson, 2014). Since then star-formation activity has been steadily decreasing. We therefore find ourselves in a rather pleasant part of the history of our universe, when the messy activity of galaxy building and star-formation has settled down to a sedate pace.

This sequence of events sounds straightforward enough, but when it comes to the details of how and why any of this really happened we, in fact, know really very little. A large part of astronomy, and extragalactic astronomy in particular, is devoted to finding out the how and the why, and figuring out what the universe looked like throughout its 13.6 billion year history. As any historian will tell you, establishing exactly what happened when is no easy task. Fortunately, the laws of physics have thrown us a lifeline, in the form of the finite speed of light. The fact that light takes time to travel from one point to another means that when we observe something we see the object as it was when the light was emitted, rather than as it may be now. For example, the Sun is about 8 light-minutes from Earth so we see it as it was 8 minutes ago (which, hopefully, is much the same as it be in 8 minutes time). So if we can catch light that was sent out from very distant galaxies a very long time ago, we can see the universe as it was then. Essentially, telescopes provide us windows into the past.

That solves it, right? Just take some pictures of the universe as it was when it was young and problem solved. Well unfortunately, or thankfully for those of us who make our living from studying this stuff, it isn't that easy. Firstly, light doesn't travel for 12 billion years through the universe completely unchanged. As the light travels, the universe keeps expanding and as it does so the light wave gets steadily more stretched, making it redder—a process simply known as cosmological redshift. This process does give us an extremely useful tool; if we can determine how big the redshift is, we can determine how far away a

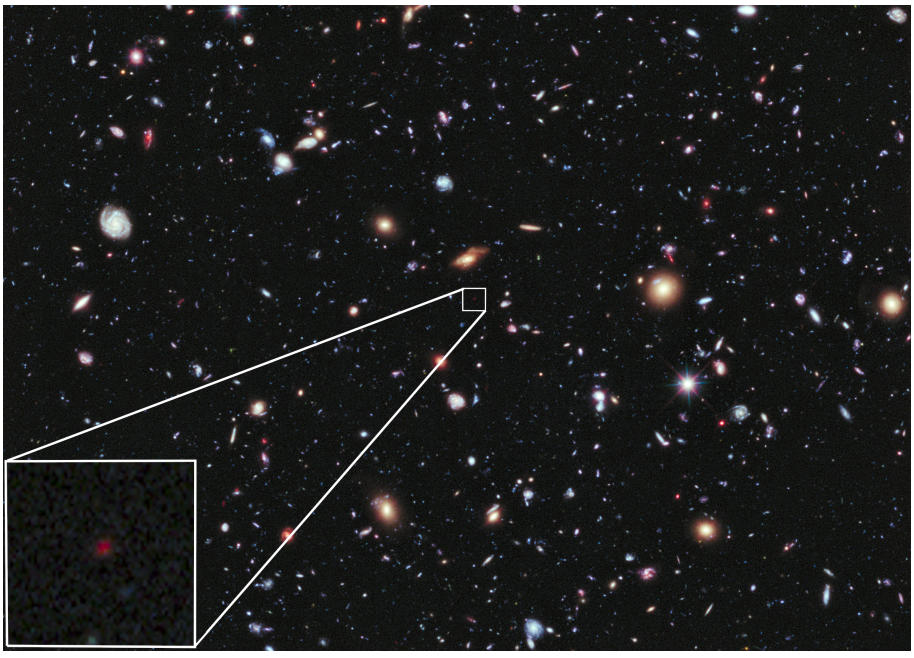

Figure 1.1: Section of the Hubble Xtreme Deep Field. Adapted from image by *NASA; ESA; G. Illingworth, D. Magee, and P. Oesch, University of California, Santa Cruz; R. Bouwens, Leiden University; and the HUDF09 Team*

galaxy is. Indeed, in extragalactic astronomy most distances are measured in redshifts (abbreviated z), and I will refer to redshifts between 0 and 0.5 as local or low redshift, and above ~ 2 as high redshift throughout this thesis.

Secondly, the light gets attenuated by the distance it needs to travel, the same way that backing away from a candle makes it appear less bright. So if we want to observe the earliest galaxies and stars in our cosmos we have to contend both with faintness and with a lot of redshift. To do this we need to collect as much light as possible—every photon is valuable. This is why we build very large telescopes (for instance the aptly named Very Large Telescope (VLT) and soon enough Extremely Large Telescopes (ELTs)).

Then what do we see when we point our ludicrously sized light buckets at the sky? Well, quite a lot and not very much depending on what and how you look at it. Figure 1.1 shows part of the Hubble eXtreme Deep Field, taken by using the Hubble Space Telescope to stare at a single pointing on the sky, that appears completely empty to the naked eye, for a really long time. All of the points of light and shapes that you see in that image are galaxies—some

relatively nearby and others supremely distant. Clearly we see quite a lot in the night sky[1]. The point that we can see very little on the other hand, is made by the inset panel which shows light from a very distant galaxy in that image. Only a few pixels of red light from a galaxy formed soon after the creation of the universe.

While essentially all points on the timeline of the universe are interesting to study in their own right, there are a few times that stand out as particularly complex and active areas of research. One such time is the Epoch of Reionization. There are many open questions about this transition. When did it start and when exactly was it complete? What sources of radiation powered it? Was the majority of the ionizing radiation supplied by superheated matter falling into supermassive black holes, which appear to reside in the centers of galaxies, or by massive stars? Were those stars located in large and rare galaxies or in smaller, more common, ones? To find the answers to questions such as these we need more information about the galaxies and their stars but, as we just noted, galaxies at high redshift are faint and hard to study. On the other hand, we can observe more local galaxies in much more detail, but how do we know if what we find applies to the galaxies in the earliest times of the universe? The work I have done in this thesis focuses on how we can use local galaxies to figure out properties of the enigmatic high redshift systems and quantifying how similar, or indeed how different they are from their low redshift counterparts.

1.1 How do we study galaxies

Now that the scene is set and we have a picture of what we want to find out, albeit a bit of a fuzzy one, a very obvious question rears its head—how do we really learn anything about galaxies, and any astronomical object and location for that matter, when they are fundamentally impossible to travel to? If I am allowed to oversimplify it for a second I would say this—we stare at the distribution of light from the object as a function of wavelength. This answer is so broad that it probably helps exactly no one and yet it does cover a very large majority of astronomical research (apologies to the cosmic ray, neutrino and gravitational wave experts who rightfully may feel left out). Let's explore it in

[1] I also refer the reader to xkcd number 2596 for a nice graphical illustration of the fact that there is a lot in the sky.

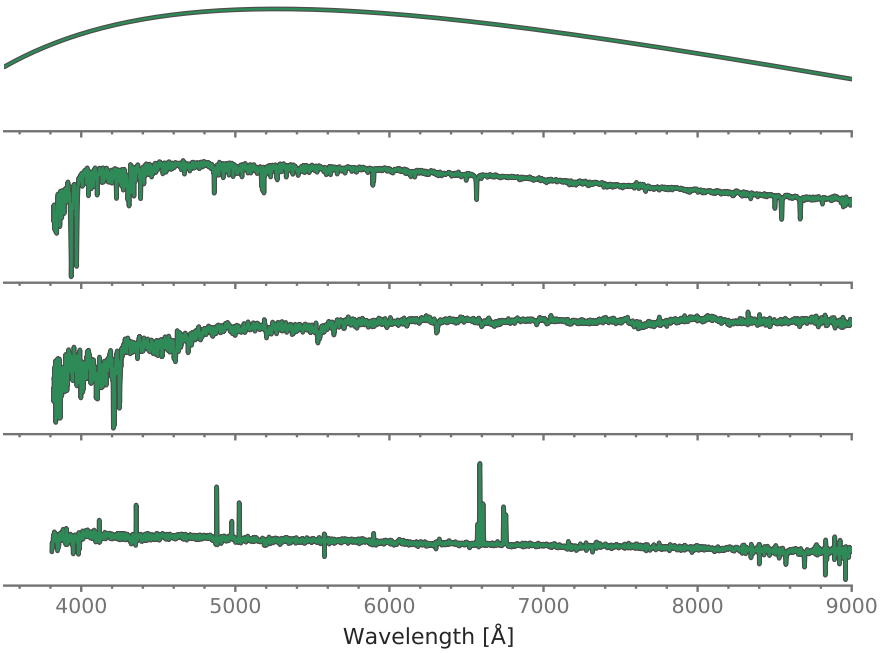

Figure 1.2: Example optical spectra of a blackbody of 5500K, a solar type star, an early type galaxy and a starforming galaxy. The Y axis is given in arbitrary units but on a logarithmic scale which amplifies the low intensity signal and lets us more fairly compare the star forming galaxy to the others despite the presence of very strong narrow lines.

a little bit more detail then.

As we split the light of an object by its wavelength into a spectrum we can look for the presence—or absence—of various features and shapes that can tell us an enormous amount about what is happening in the system. Figure 1.2 shows a compilation of spectra of the optical light from 4 different sources. The first spectrum is a simple blackbody—the light distribution that you get from an idealized object with a specific temperature (in this case 5500K, the same temperature as the surface of the Sun). The second spectrum is that of a solar type star. It is immediately quite clear that stars are pretty well approximated by simple blackbodies but that there is something more going on leading to lots of little bumps and spikes—spectral lines. Each of these lines comes from the presence of a particular element or molecule in the atmosphere of the star.

The next spectrum is now no longer just a single star but in fact an en-

tire galaxy, in this case an old and evolved galaxy that is no longer forming new stars. (This type of galaxy is incidentally known as an early type galaxy which is another one for the list of strange and counter-intuitive astronomy terms.) This spectrum still resembles that of a single star but of lower temperature—moving the peak of the emission to longer wavelengths—since older and colder stars dominate the light of these kinds of systems. The last spectrum in the figure is much more closely related to what I study in this thesis, which is that of a star forming galaxy. This spectrum is quite different. We see that the general shape of the spectrum is different, being dominated by strong and narrow spectral lines. The flux is shown in log scale to let us see the continuum at all, and we can note that the peak of the continuum for this galaxy lies further to the blue than the spectrograph can reach. The immensely strong spectral lines are being formed in the gas between the stars when it is ionized by young massive stars.

The interstellar gas or interstellar medium (ISM) is enormously complex with many active physical processes, from ionization to large scale motions, shocks and winds. These processes combined with the different elements present in the ISM together give rise to many spectral lines and features. If we can identify them and measure their strengths relative to each other and relative to the underlying light from the stars, we can figure out what the conditions are in the gas where they are created. This sounds very easy but in reality it is, of course, fraught with difficulty. However, there are now many emission lines where the atomic physics are well understood or models and calibrations exist that allow us to make quite detailed statements about galaxies and how they work. Perhaps the most studied spectral range is the optical, which roughly corresponds to the wavelengths that we can see with our eyes. Optical light is in fact very informative for several reasons—firstly because it is easily transmitted by our atmosphere, which means we can use large ground-based telescopes to measure it, and secondly because it contains a large amount of very prominent emission lines. For instance, perhaps the most commonly used emission line is that of Hα, a spectral line produced when ionized hydrogen recombines with an electron. The ionized gas that produces this line is formed around short-lived massive stars and so the strength of the Hα line is frequently used as a measure of the star formation rate of the galaxy. Another is the Lyα line which lies in the UV part of the spectrum and is the primary

focus of this thesis.

1.1.1 Why are we studying UV lines in particular?

There are a few reasons for studying specifically UV emission from galaxies. One of the strongest is that, as I mentioned in the very beginning of this chapter, light from the early universe is strongly redshifted—the wavelengths from redshift 10 are 11 times longer now than they were when emitted. This means that our ordinary optical lines and diagnostics now have wavelengths that are inaccessible even to space telescopes that observe quite far in the infrared (IR), such as the James Webb Space Telescope (JWST). And they certainly cannot be observed from the ground since the atmosphere is not transparent to this IR radiation. This means that UV light will be one of the very few accessible sources of information about the earliest galaxies. Learning anything about these galaxies then requires that we understand the processes that produce and alter UV emission lines and spectral features. The work that is presented in this thesis aims to do this by using UV observations with the Hubble Space Telescope of nearby galaxies where we can get all the ordinary optical lines to compare with and also spatially resolve the structure of the galaxy.

1.1.2 Why is Lyα especially interesting?

In this thesis I focus on the Lyα line of hydrogen which is, as we noted, a UV emission line. However, it also has another interesting property, namely that it is a resonant line. We will talk about what this really translates to in terms of physics in the Chapter 3, but in brief it means that Lyα light can bounce off neutral hydrogen atoms. When a light particle, a photon, from an emission line that isn't resonant encounters an atom which it can excite it does so, and then the atom emits a series of photons in other wavelengths as it de-excites. On the other hand when a resonant emission line excites an atom there is only one pathway by which the atom can de-excite: by emitting a photon of the same wavelength as the one that was absorbed. Seen from the outside, a Lyα photon encounters a hydrogen atom and an identical photon is then re-emitted in some new direction.

Well so what? We end up with the same photon again—can't we just ignore this and get on with our lives? Well, it turns out that the photon is

not necessarily exactly identical, there is a chance that it carries a tiny bit of information about the scattering atom away with it. Looking at a large amount of individual photons this tiny effect can lead to some very interesting emission line properties.

The UV wavelength coupled with resonance and intrinsic brightness of Lyα is a potent combination and makes it a potentially extremely versatile astrophysical tool. We can use it to find the most distant galaxies known and study the neutral gas that surrounds them. By looking at how Lyα is lost in the thin gas lying between galaxies at the very highest redshifts, we can map out the progress of the Epoch of Reionization. As if this wasn't enough to warrant us studying Lyα, the conditions that let Lyα escape from a galaxy also favor the escape of ionizing radiation, meaning we can potentially use Lyα to find out what sources powered that reionization process.

One of the core ambitions and hopes of the work in this thesis is that we could use the versatility of Lyα to better understand galaxies, the neutral gas that surrounds them, and potentially even the gas that fills the voids between them.

2. Cosmic history & galaxy evolution

The field of extragalactic astronomy has progressed at high speeds in recent years, but the history of the universe is long and complex and many open questions remain. In this chapter I try to give a brief summary of the current state of knowledge of large scale cosmic evolution, galaxy evolution, and some of the major unknowns, as well as how my research can help with filling these gaps.

2.1 The first stars and galaxies

After the initial nucleosynthesis and inflation period of the universe the universe entered a period known as the Cosmic Dark ages, before the formation of any stars or other structures we would recognize from our current universe. This dark age did not last very long however. As gravity acted on the fluctuations in the dark matter, it began to clump—dragging the hydrogen and helium gas with it—and causing the formation of the first stars. This process started around a redshift $\gtrsim 20$, a few hundred million years after the Big Bang (Greif, 2015). The first stars are often referred to as Population III stars (Pop III)[1] and the process of their formation was quite unlike what we observe today (Abel et al., 2002; Bromm, 2013; Bromm et al., 1999, 2002) due to the lack of metals in the gas. These stars were metal free and likely very massive causing them to emit substantially more ionizing radiation than the stars we observe today. Their large masses also mean that they were also most likely short lived (see e.g. Murphy et al., 2021). The impact of these stars on the environment was immediate and profound—ionizing the gas and enriching the surroundings

[1] The reason for the name is that the types of stellar populations are named based on their metal content with Pop I being young blue stars in the Milky Way, Pop II being older, more metal poor, stars, and Pop III being the first, metal-free, stars.

with metals.

The formation of the first stars also heralded the beginning of galaxy formation and evolution. It is commonly accepted that galaxy formation proceeds in a hierarchical fashion, with small building blocks—such as the Pop III stellar associations—coalescing and forming larger galaxy structures, eventually producing the large spirals and elliptical systems that we observe in the local universe. However, the detailed properties of the first galaxies and how they were structured is still unknown and due to their high redshift ($z \sim 30$, Bromm, 2013) they have been observationally elusive.

2.2 The Epoch of Reionization

As galaxies and stars formed they also started to ionize the surrounding intergalactic medium (IGM), marking the transition into the Epoch of Reionization (EoR). The EoR stretched from the formation of the first stars all the way to redshift (z) between 6 and 5 when essentially all the hydrogen in the intergalactic medium (IGM) is ionized (Fan et al., 2006; McGreer et al., 2015) . The EoR is the last large-scale phase-transition of the universe and consequently of great scientific interest. While it is very clear that the universe went through this transition from measurements of the cosmic microwave background (CMB, e.g. Planck Collaboration et al., 2016), some quite fundamental details of the transition remain difficult to constrain. These range from the exact spatial structure and timeline of the process to which sources powered it.

There have been many different methodologies designed to extract as much information as possible about this transition from many different kinds of observations. Since it relates to the spatial distribution of neutral hydrogen, the most intuitive source of information is emission from the 21 cm transition of neutral hydrogen. However, detecting this signal is extremely challenging and requires the next generation of large radio telescopes, i.e. the Square Kilometer Array (SKA, Mellema et al., 2013). In lieu of direct observations we then have to use more indirect tracers such as the CMB, absorption line studies of quasar spectra, or observations of star-forming galaxies. Part of the work I present in this thesis is directly related to this latter point.

Each of these indirect methods have their own set of limitations and provide complementary views on the reionization process. For instance, CMB

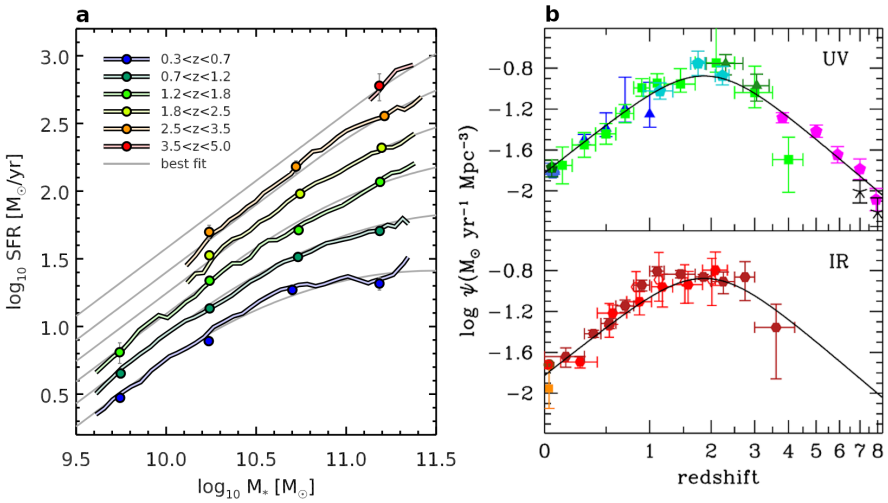

Figure 2.1: Panel **a** from Schreiber et al. (2015) illustrates the relation of star-formation rate with stellar mass for galaxies between redshifts 0.3 and 5 based on HST and Hershel observations of 62 361 galaxies. Panel **b** from Madau and Dickinson (2014) shows the star formation history of the universe as traced by UV and IR radiation.

measurements can only really determine some global reionization quantities such as the redshift of the mid point of reionization. On the other hand Lyα absorption in quasars are only sensitive to the end of reionization since the absorption becomes saturated at low IGM neutral hydrogen fractions. Observations of star-forming galaxies offer the opportunity of tracing the detailed evolution of the IGM neutral fraction further into the EoR.

2.3 Cosmic noon and the main sequence of galaxies

During the EoR the mean star-formation rate (SFR) of the universe kept increasing (Ellis et al., 2013; Madau and Dickinson, 2014, see Figure 2.1**b**), and galaxy formation was ongoing. This increase continued rather steeply all the way to redshift ~ 2, also known as cosmic noon. At this point of intense star-formation the universe was making new stars at 8 times the rate that we observe in our local galactic neighborhood (Madau and Dickinson, 2014). However, the cosmic average only tells part of the story, and if we want to understand the sequence of events on a more detailed level we need to understand how individual galaxies looked and functioned at these times.

The SFR of an actively star-forming galaxy is quite closely related to its mass, a relation that is often referred to as the main sequence of galaxies[1]. If star-formation proceeded in the same environments and in the same conditions throughout cosmic history, we would expect this main sequence to be constant. However, it is not. Figure 2.1**a** shows the change in the main sequence as a function of redshift from Schreiber et al. (2015). It is quite apparent that star-formation was more "intense" at early times, i.e. the specific star-formation rate (SFR divided by stellar mass) was higher (see e.g. Ilbert et al., 2015; Leslie et al., 2020). Clearly the high-z environments with ongoing galaxy formation, merging, and growth, yield quite extreme environments.

If we then wish to understand early, primeval, galaxies in detail, we have essentially two options. The first is to directly observe them. While this is conceptually simple, it is very difficult in practice due to the extreme distances to these galaxies, causing redshifting of galaxy light, light attenuation by distance (proportional to the distance squared), and cosmological surface brightness dimming (proportional to $(1+z)^4$). The other way is to identify galaxies that appear to be similar to high-z galaxies but lie at much lower redshifts where their physical processes can be studied in great detail. One challenge in this case can be readily understood from the main sequences in Figure 2.1—since galaxies at high-z in general are so extreme, comparable galaxies at low-z are very rare. Another challenge is to know whether the galaxies we are studying are really true analogs of high-z systems.

The work in this thesis is concerned with low redshift galaxies, understanding what insights we can extract from them, and if and how they differ from their high-z counterparts.

2.4 Why Lyα?

The primary topic of study in the work I present here is emission from the Lyman α spectral line of hydrogen. While I will discuss the details of this emission line in the next chapter I think it behooves us to spend a little bit of time motivating why Lyα in particular deserves such attention.

In recent years, Lyα has proven to be an extraordinarily useful astrophysi-

[1] Although, there has been some disagreement about this terminology since the SFR-mass relation is not really an evolutionary sequence

cal tool for several reasons. Lyα is a quantum-mechanically allowed transition from the ground state to the first exited state of the hydrogen atom, which—combined with the prevalence of hydrogen in the universe—means that it is intrinsically the strongest emission line from astrophysical nebulae (Dijkstra, 2019). When this fact is combined with the UV wavelength of the line, it becomes clear that Lyα holds great promise as a tool for discovering galaxies at high-z since it redshifts into the optical and becomes observable from the ground at about redshift 1.5. This use of Lyα was proposed already by Partridge and Peebles (1967) and has now been used on a grand scale with projects such as MUSE-Wide (Urrutia et al., 2019), Silverrush (Ouchi et al., 2018) and HETDEX (Lujan Niemeyer et al., 2022), discovering thousands of galaxies by their Lyα emission.

However, interpreting Lyα observations is not trivial. This is because it is a resonant line. A resonant emission line is a line that when absorbed by an atom is re-emitted back in the same transition—in this case a Lyα photon can be absorbed by a neutral hydrogen atom, but there is then only one main de-exitation pathway for the atom: the emission of a new Lyα photon. This means that Lyα effectively scatters on neutral hydrogen, of which there is plenty in galaxies. As we shall see in the next chapter this drastically affects both the wavelength distribution and spatial emission patterns of Lyα.

However, it also means that instead of just tracing the ionized medium where it is produced, Lyα can potentially also be used to make inferences about the neutral hydrogen medium—specifically the neutral hydrogen between galaxies, in the circumgalactic (CGM) and intergalactic (IGM) media. If we can understand the resonant scattering patterns and mechanisms of Lyα we could then shed light on many important areas, for instance the CGM reservoir of gas that accretes into galaxies and powers their star-formation, or even the progression of the neutral fraction of the IGM during the EoR.

3. Hydrogen emission lines

As I noted before, resonant emission lines have some particular properties that make them both interesting to study and complex to interpret. They also make them potentially very powerful tools for understanding things about our universe that may otherwise be hard to get at. The following chapter examines the physics of emission from the hydrogen atom and the resonant Lyα emission line in particular. The aim is to clarify how resonant emission lines works, and what this means for interpreting observations of them and how they can be useful for studying galaxies. Specifically, I start by looking at how and where the hydrogen line photons, including Lyα, are produced and then I talk about what happens when Lyα encounters neutral hydrogen.

3.1 Production of Lyman alpha photons

3.1.1 Hydrogen emission lines

Lyα is intrinsically the strongest spectral line of hydrogen, and in fact the strongest spectral line overall when considering astrophysical nebulae. This is because Lyα photons are produced during the transition from the first exited state to the ground state of the hydrogen (H) atom, which is the most common element in the universe. A simplified illustration of the energy level structure of the hydrogen atom is shown in figure 3.1. Lyα is the first line in the so called Lyman series of transitions, i.e. transitions to the ground state of the hydrogen atom. The second line in the series, Lyβ is the transition from the second excited state, Lyγ from the third etc. Transitions down to the second level of the atom are known as the Balmer series of transitions—the most well known of these transitions is Hα which we will discuss in many places since it is a very useful diagnostic that can tell us much about both star-formation in galaxies, and, as we shall see, the intrinsic production levels of Lyα.

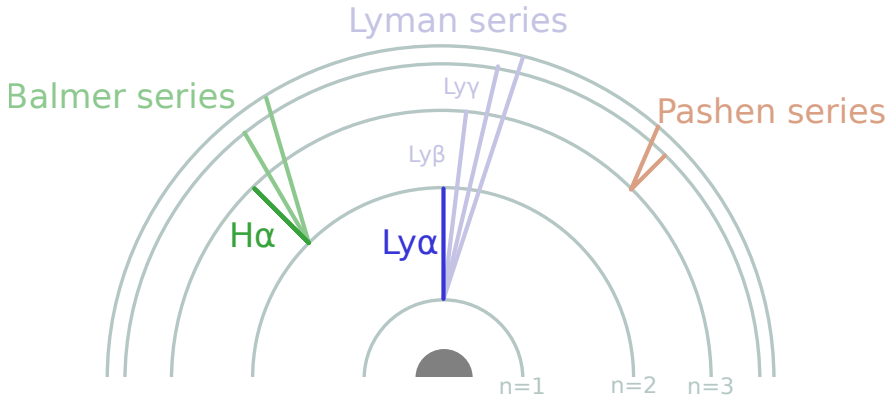

Figure 3.1: Figure schematically illustrating some of the energy levels of the hydrogen atom and the Lyman, Balmer, and Pashen series of transitions. Longer transition lines correspond to higher energies and, consequently, shorter wavelengths.

3.1.2 Origin of Lyα photons

Lyα emission happens as part of a series, or cascade, of transitions as an excited hydrogen atom de-excites down to its ground state. There are two primary pathways for this excitation to happen: recombination after ionization and collisional excitation. In principle it is also possible for absorption of continuum photons that lie at the wavelengths of higher order Lyman series to excite the atom and produce Lyα—a process known as continuum pumping (Baker et al., 1938; Ferland, 1999; Luridiana et al., 2009). However, this process is not efficient and is usually negligible compared to recombination radiation which I will discuss next, so I will not consider it further here.

The primary source of Lyα in actively star-forming galaxies is recombination. This is due to the presence of young massive stars that produce copious amounts of photons capable of ionizing the interstellar gas. As the ionized hydrogen atom nucleus (which is just a proton) recombines with a free electron, the reformed atom ends up in an excited state. The electron then rapidly falls back down to the ground state and emits photons, often including Lyα as it does so. In principle, an electron could recombine directly into the ground state of the atom, however, the excess energy of the electron is then converted into a photon that can ionize another nearby hydrogen atom, and does so almost immediately. This means that in most astrophysically relevant cases this

process can be safely ignored. This approximation is known as the on-the-spot approximation and means that the only relevant recombination events are the ones that leave the electron in an exited state from which it falls down through the energy levels, emitting photons as it does so. This is known as a radiative cascade.

Given some assumptions on the state of the gas, it is possible to calculate in what percentage of events the cascade results in emission of a Lyα photon. Assuming a gas temperature of around 10^4K and densities that are low enough that collisions do not dominate, roughly 68% of all ionizing photons are converted to Lyα via ionization and recombination (Dijkstra, 2019). Under these assumptions, which tend to hold rather well in most astrophysical contexts, the Lyα and Hα ratio is also set by quantum mechanics. While the ratio depends on the exact density (see for instance Dopita and Sutherland (2003) and Henry et al. (2015)), it is commonly taken as intrinsic Lyα being equal to $8.7 \times$ Hα. Hα can therefore be used to estimate the fraction of Lyα photons that escape a given environment which, as we shall see later, is very important.

The other possible source of Lyα is collisional excitation, which occurs when a hydrogen atom collides with a free electron without recombining. The electron can then transfer some of its kinetic energy to the atom which is subsequently lost via radiative de-excitation. Such an event essentially converts the kinetic energy of the free electrons into radiation, causing the gas as a whole to cool. It is therefore commonly known as cooling radiation. Since the emission mechanism here relies on free electrons interacting with neutral hydrogen (HI) atoms the probability of this process occurring is directly dependent on the density of the gas, since higher density leads to greater likelihood of collision. The rate of Lyα production by collisions is also a function of the temperature. Finding the exact temperature dependence is not a trivial problem due to the complexities of quantum mechanical effects (Dijkstra, 2019). It has been shown that the cooling function of neutral hydrogen, including all line emission, not just Lyα, peaks at $T \sim 10^{4.2}$K (Dijkstra, 2019). This type of cooling via Lyα is expected to be important for the accretion of pristine gas onto galaxies via cold streams and similar processes (Barnes et al., 2014) and could be a source of faint and extended Lyα emission (Dijkstra and Loeb, 2009; Fardal et al., 2001; Goerdt et al., 2010).

3.2 Resonant scattering and Radiative transfer

The fact that the Lyα transition is from the ground state means that a Lyα photon has enough energy to excite a neutral hydrogen atom. The excited atom however, has only one main de-excitation pathway—through the emission of another Lyα photon. This means that in principle Lyα photons can be absorbed and re-emitted a virtually infinite number of times by HI atoms without the energy being converted to anything but another Lyα photon. If we, for simplicity, consider each re-emitted photon to be the same as the original photon that was absorbed, we can describe this process as Lyα radiation bouncing, or scattering, on neutral hydrogen gas. As we mentioned before, a photon that has this property is often referred to as a resonant photon.

The resonance would not be of any great consequence if the probability of a Lyα photon interacting with an HI atom were low. Interaction probabilities of atoms and photons are set by quantum mechanics and are usually talked about in terms of cross-sections. The quantum mechanical cross-section essentially describes how "big" the atom appears to the photon.

If the absorption cross-section of Lyα with HI was small, Lyα photons would simply pass the hydrogen atoms by and be none the wiser. However, Lyα is a quantum mechanically allowed transition which means that the cross-section is *very* large—on the order of $\sigma \sim 5.9 \times 10^{-14}$ cm^2 at 10^4K at line center (Dijkstra, 2019). This number may look small and it is indeed difficult get a sense of how large it is without some comparisons. For instance, the maximum cross-section for a Lyman continuum (LyC) photon, i.e. a hydrogen ionizing photon, is 6×10^{-18}. Another example is the Thomson cross-section for interactions between free photons and electrons which is roughly 11 orders of magnitude lower than the Lyα cross-section (Dijkstra, 2019) and still an important astrophysical process. To continue the size analogy—the hydrogen atom will appear 10000 times larger to a Lyα photon than to LyC photon, and 10^{11} times larger than a free electron. Translated into optical depths the cross-section means that a Lyα photon encounters an optical depth of $\tau = 1$ for an HI column density of 10^{14}cm^{-2}. This value, again, does not mean much on its own so we note that average HI column densities of star forming galaxies tend to be of the order of 10^{19}(Kalberla and Kerp, 2009, based on Milky Way measurements) or greater. The optical depths for an average Lyα photon

is therefore around 10^5 or 10^6. This means that for a Lyα photon to escape a galaxy and be observable by us, it has to traverse a very highly optically thick medium. In fact, even ionized regions can be optically thick to Lyα at line center since they have a residual neutral fraction due to the recombination and ionization balance. The exact value depends on the density structure and radiation field but is often quoted as $\sim 10^{-4}$. However, the cross-section is also very sensitive to the exact wavelength of the photon, which turns out to be very important later.

It would intuitively seem that this means that we should never observe Lyα from astrophysical sources, and without resonance essentially no radiation would escape from such an optical depth. However, because Lyα is not destroyed in interactions with HI, escape of Lyα photons is still possible, and indeed we do observe it from many galaxies as we shall see in the coming chapters.

The Lyα photon is not entirely unchanged when scattering from atom to atom. Firstly, purely quantum mechanical randomness means that the photons may be re-emitted with a frequency that is shifted from the central wavelength. Secondly, the scattering atoms are not stationary, and their velocities (due to either thermal motions or bulk motions in the gas) also leave frequency shift imprints on the Lyα photon. The combined probability distribution of thermal and quantum mechanical effects is described by the Voigt-distribution which combines a thermal, Gaussian, core with the strong wings of a Lorentz distribution.

When the photon receives a frequency shift, the cross-section to interact with new hydrogen atoms changes which consequently reduces its apparent optical depth, essentially shifting it out of resonance. Additionally, the presence of, for instance, dust can cause Lyα photons to be absorbed and lost. In order to know how Lyα escapes an HI cloud we must describe how these processes work in more detail—it needs to be treated as a full radiative transfer problem. The mathematical base of this is the radiative transfer equation, which describes how radiation travels through a medium and how the intensity along a sightline is affected by processes in the medium. I show the equation below but I will not go into the details of the mathematics, instead I qualitatively describe the three main terms that enter into the expression and how they impact Lyα.

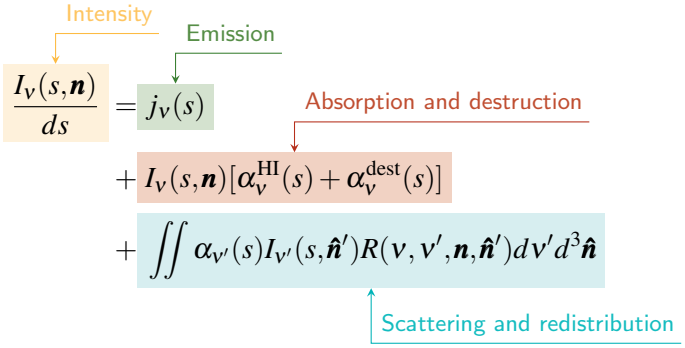

Emission The first term of the radiative transfer equation describes the fact that each part of the gas that the light travels through may add new photons to the light. The main contributions to this term come from recombination and collisional excitation with its subsequent de-excitation, as discussed previously.

Destruction The second term of the equation describes how the incident radiation is absorbed and destroyed in the gas parcel we are considering. There are a number of effects that enter into this term but the primary ones are absorption by dust and interaction with molecular hydrogen (Dijkstra, 2019). Absorption of a Lyα photon by dust grains reprocesses the Lyα into thermal emission in the infrared. This effect is very important even when the amount of dust in the medium is low due to the long escape path that Lyα suffers as a result of the resonant scattering. We discuss this further below.

Lyα can also be destroyed in media with large concentrations of molecular hydrogen. The reason for this is that this molecule happens to have an energy transition that lies very close to the restframe Lyα frequency. This means H_2 can absorb Lyα photons, but there is then another pathway where instead of re-emitting a Lyα photon, as an HI atom would, the energy is converted into vibrational line emission.

Redistribution This last term describes how Lyα scatters, both in space and in frequency along the path. This term is the most complex and is also at the root of why Lyα radiative transfer is a non-trivial and interesting problem. The detailed properties of this term dictate the impact that interaction with HI atoms has on the Lyα photons in terms of im-

parted frequency shifts both away from and towards line center. Since such interactions happen in virtually every environment, this term has a substantial impact on the properties of the Lyα radiation we observe from emitting objects. Additionally, since this term describes frequency shifts, it also determines how many scatterings a photon undergoes and how far it needs to travel before escape.

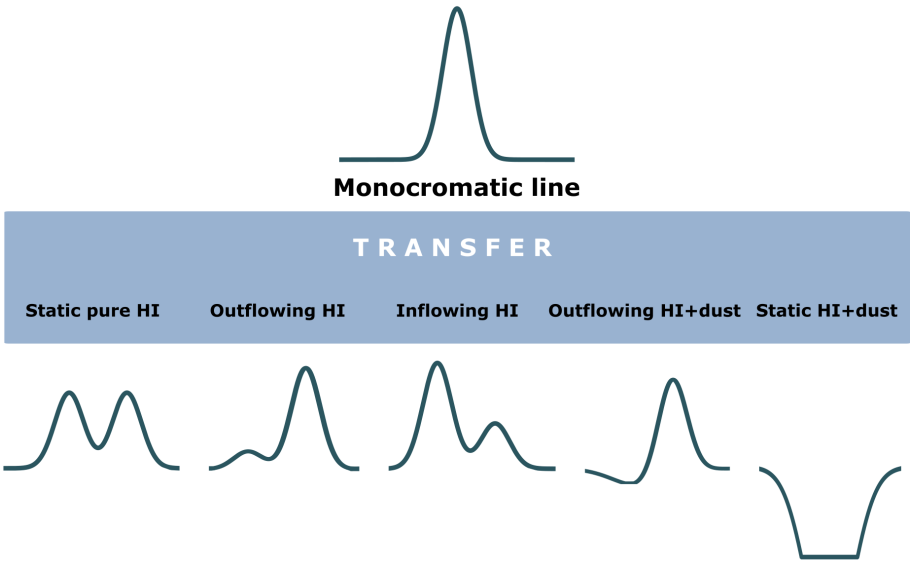

Figure 3.2: Schematic figure illustrating the effect of radiative transfer on a simple input Lyα line. The effects of the transfer and redistribution are very varied depending on the exact gas properties and range from complete absorption of the line to double peaks with various line strengths.

The redistribution component transforms simple monochromatic line radiation into a complex array of spectral and spatial profiles. Some synthethic examples of this are shown in Figure 3.2, and see Chapter 6 for some observed examples. This means that this term, known as the redistribution function, warrants some additional attention. I will discuss the function in more general terms and illustrate the behavior of the function in some specific cases. For a full treatment of the mathematics see Dijkstra (2019).

The redistribution function essentially maps from a photon travel direction and frequency before the scattering event, to a new travel direction and frequency after the scattering event. Some examples of what this redistribution

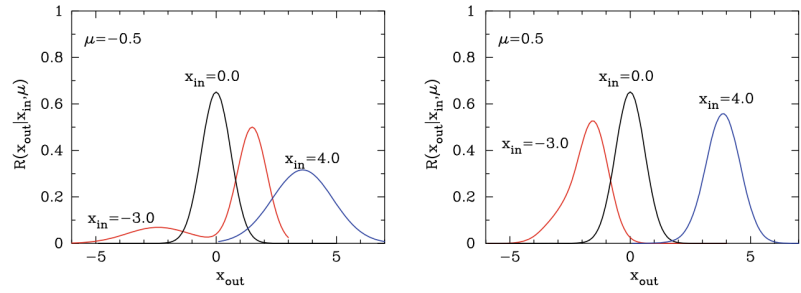

Figure 3.3: Figure from (Dijkstra, 2019) showing the probability of an output frequency $x_{\rm out}$ after scattering for a given input photon frequency $x_{\rm in}$ and infall direction μ. The frequencies are given in dimensionless frequency units, which is defined as frequencies relative to line center in units of the thermal doppler frequency (see e.g. Barnes et al., 2014; Dijkstra, 2019).

function can look like are shown in Figure 3.3 where each curve describes the probability of an output frequency given an input frequency $x_{\rm in}$ and a scattering angle μ (i.e. the angle between the velocity vectors of the photon and atom). The two panels describe two different infall angles. As we see, for example by comparing the red curves in the left and right panels, different specific combinations of $x_{\rm in}$ and μ can give quite different resulting probabilities both in terms of where the peak of the probability distribution lies, and also how broad it is. However there are also situations where the complexity of the redistribution function can be significantly reduced. In the specific case of isotropic Lyα and no dust, the radiative transfer equation can in fact be rewritten in the form of a diffusion equation, which leads to a very instructive way to think about the radiative transfer process. We can consider it as a double diffusion process in space and frequency—essentially the transfer smooths Lyα out in space and shifts the photon frequencies away from the central wavelength.

As they scatter some of the photons receive large frequency shifts away from the core, sometimes referred to as a frequency excursion. Since these photons are far from the resonance their mean free path increases greatly and they travel much further before scattering again. A simple schematic random walk is shown in Figure 3.4. I simulated the scattering process by making the scattering direction at each step uniformly random and making the step length proportional to a random sampling from a Voigt function centered on 0. While it does not quite capture the true physics of the scattering of Lyα, it illustrates

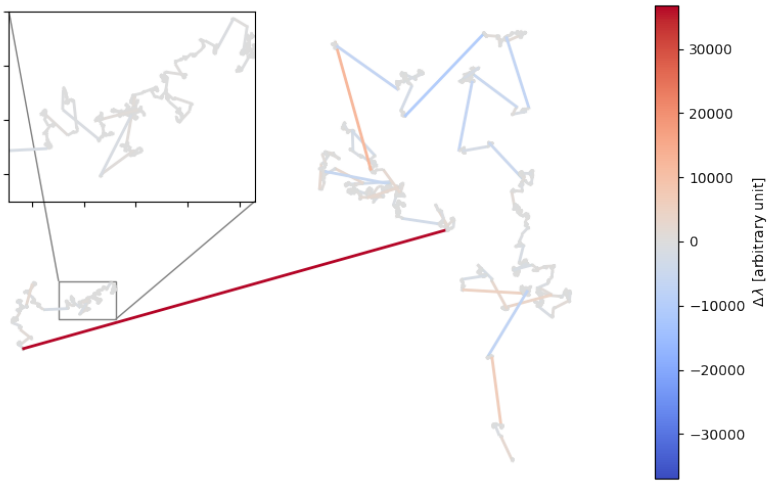

Figure 3.4: Simple random walk experiment showing what it looks like when the path-length of a Lyα photon is dependent on how far from the line core the photon has scattered in wavelength.

what the scattering process looks like, with photons with larger wavelength excursions being able to travel significantly further.

If photons with a large frequency shift scatter again they are likely to receive a frequency shift back toward the core of the line, causing the mean free path to drop significantly—essentially trapping the photons in the same spatial position until they randomly receive another large frequency shift. This process continues until escape, which means that it is very unlikely that the escaping Lyα photon has a frequency that is close to line center.

Figure 3.4 illustrates well that Lyα photons take far from the shortest path when escaping a medium. If the gas Lyα transfers through is just pure HI gas this smooths out the Lyα in space and redistributes it away from the central frequency, but if there is dust in the gas it is a different story. In this case there is a chance for a photon to be absorbed and destroyed, and the probability of encountering a dust grain directly depends on the path length the photon has to travel. It is clear that, while any photon risks absorption, scattering greatly amplifies the risk for Lyα. How important this effect is in actual systems is a matter of some debate as we shall see in the next chapter.

This discussion raises another question: If we have the radiative transfer equation, do we not have everything we need to model and understand Lyα?

In theory—yes, but in practice—no. The reason is that Lyα transfer happens on scales that are much too small to model in simulations. In fact, for a Lyα photon at line center in an HI medium of typical warm neutral ISM densities (0.5 particles cm^{-3}) the mean free path corresponds to a distance only of the order of 20 AU. This is about the radius of the orbit of Uranus, and this scale will never be resolvable in a simulation of an entire galaxy which contains billions of stars. We are then left with trying to make sense of Lyα using simplified simulations and—crucially—observations. Indeed, one of the core aims of the work in this thesis is to use observations of Lyα to investigate the scattering process and clarify which Lyα interactions with its surroundings are in fact the most important.

4. Lyα measurements and correlations

This chapter delves into the history of Lyα measurements and specifically focuses on the "global" properties of Lyα. By global in this context I refer to the total properties across a whole galaxy and integrated across the whole Lyα spectral line. We will look more into the spatially and spectrally resolved observations in the subsequent chapters.

One goal of Lyα observations from the very start was to observationally determine how much Lyα typically escapes from a galaxy and how that quantity relates to other properties of the galaxy. This problem quickly turned out to not have a single simple solution and as observations have improved and progressed, more and more properties seem to have some relation to Lyα line escape. Trying to determine the relative importances of variables and how well they relate to Lyα is the main prospect of **Paper I**.

Lyα was proposed as a potential observational marker of galaxy formation as early as 1967 by Partridge and Peebles (1967) based on simple calculations of galaxies forming by monolithic collapse. However, observations of Lyα did not start in earnest until the launch of the *International Ultraviolet Explorer* (IUE) satellite in 1978. This UV satellite was equipped with a low resolution (R[1]$\sim$250-400) spectrograph which was used by several teams in the following years to observe Lyα spectra, initially of quasars and later of star forming galaxies (e.g. Hartmann et al., 1988; Meier and Terlevich, 1981; Wu et al., 1983). It was almost immediately clear that the observed Lyα luminosities were significantly lower than the value implied by the observed Hα and Hβ luminosities and standard recombination theory. This caused some significant discussion as to whether the lack of Lyα could be explained simply by normal absorption by dust or whether radiative transfer causing preferential

[1]Resolving Power $R = \frac{\lambda}{\Delta\lambda}$

absorption of Lyα (see Chapter 3) was required. One of the earliest studies, (Wu et al., 1983), was in fact not able to reconcile the low Lyα values with the dust extinction measured from the Balmer recombination lines (i.e. Hα, Hβ). Similar results were obtained for starburst galaxies (Giavalisco et al., 1996; Hartmann et al., 1988).

Box 4.1: Common global Lyα observables

$L_{Ly\alpha}$ The total Lyα luminosity of a given target integrated over a large aperture.

$f_{esc}^{Ly\alpha}$ Escape fraction of Lyα. Defined as the observed Lyα luminosity divided by the intrinsic Lyα luminosity. The most common way of estimating the intrinsic Lyα luminosity is to use observations of Hα and the fact that for normal ISM gas temperatures and densities the Hα / Lyα ratio is given by quantum mechanics and is ~ 8.7.

Lyα EW The Lyα equivalent width (EW) is defined as the Lyα flux over the local continuum flux density, i.e. the integrated emission line flux described in units of the local stellar emission.

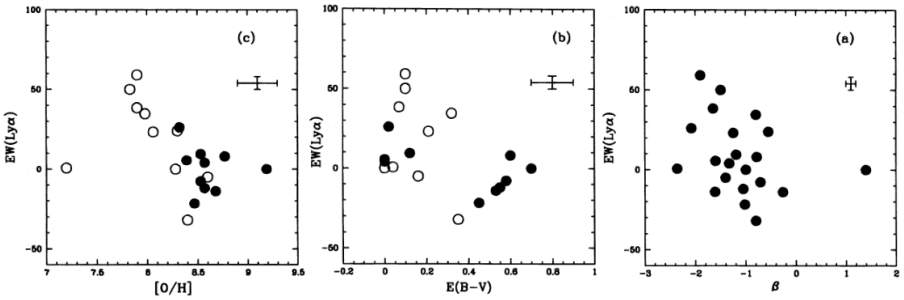

Figure 4.1: Correlations of Lyα EW with galaxy properties. Adapted from Giavalisco et al. (1996). Open and filled circles simply show different sources for the optical spectra used. The first panel shows the correlation between Lyα EW and metallicity, the second with dust, and the third with UV slope (β). Notably, all correlations are quite weak.

These findings led to a quite extensive debate on whether additional dust extinction from the resonant scattering of Lyα were required to explain the observed line ratios. Calzetti and Kinney (1992) concluded that the escape fractions that they observed could be explained from just pure dust extinction

without the need for additional extinction. Giavalisco et al. (1996) performed a reanalysis of 21 spectra obtained with the IUE and found that the correlation with dust was almost absent and the correlation with metallicity that had been previously reported was substantially weakened. The main correlation plots from that work are shown in Figure 4.1. From this they concluded that the escape of Lyα should be mostly controlled by the geometry of the ISM and how dust was distributed in it rather than how much dust was present. A similar conclusion was reached by Scarlata et al. (2009) after considering different geometrical distributions for the dust. They found that while the extinction from a simple dust screen in front of the emitting source could not reproduce the observed line ratios between Lyα and Hα, a clumpy dust screen could. These observations implied that Lyα escape would be mainly controlled by dust, but the small samples made this conclusion tenuous.

Atek et al. (2009) studied a sample of Lyα emitting galaxies selected from *Galaxy Evolution Explorer* (GALEX) observations and found that the Lyα escape fraction ($f_{esc}^{Ly\alpha}$) again showed an anticorrelation with the dust extinction. However, they also noted that there was significant scatter around the correlation, suggesting that more parameters than just dust are in play. An additional study of the dust correlation with Lyα was presented by Mallery et al. (2012) who examined high redshift ($4.2 \leq z \leq 5.6$) galaxies and came to the conclusion that dust extinction is the most important regulating parameter for the escape fraction, based on the fact that when a galaxy shows high extinction it also shows low $f_{esc}^{Ly\alpha}$. However, they also noted that at low extinctions $f_{esc}^{Ly\alpha}$ was significantly more unconstrained. So, according to Mallery et al. (2012), it seems that at low Lyα escape fractions dust extinctions appear insufficient to explain the attenuation while at high escape fractions one would have expected more attenuation than is observed.

Clearly, despite some intriguing correlations, dust is not the end of the story, and we are forced to examine other correlations if we want to find the source of the scatter. One correlation, or rather anticorrelation, that was quite clearly seen in the early samples was between the metallicity of the galaxy and Lyα escape fraction (Hartmann et al., 1984, 1988; Meier and Terlevich, 1981; Terlevich et al., 1993) with lower metal content of the ISM gas often corresponding to higher $f_{esc}^{Ly\alpha}$. The exact mechanism that would cause such a correlation is not quite clear since metals in the ISM do not directly influence

Lyα (Hayes, 2019) but they can affect several processes that do. For instance, metal content should correlate with dust present in a galaxy since metals are the building blocks of dust. They could also impact the production of Lyα by affecting the output of ionizing photons from massive stars (Leitherer et al., 1999). As we discuss in more detail in Chapter 6.5, we also find a strong metallicity correlation in **Paper V**. However, it was quite quickly found that low metal content is not a sufficient condition for a galaxy to be a strong Lyα emitter. Thuan et al. (1997) observed the very metal-poor galaxy SBS 0335-052 and instead of the expected emission they found a very broad and strong Lyα absorption feature.

Later studies, such as Kunth et al. (1998), pointed out the potential importance of ISM kinematics by noting the fact that even a very small amount of dust can suppress Lyα highly effectively if it is contained in a static medium and therefore large scale gas motions, such as outflows, should play an important role in regulating Lyα escape. Mallery et al. (2012) found something similar, concluding that if there is sufficient dust present in a galaxy Lyα cannot escape regardless of kinematics or neutral gas content whereas if there is only a limited amount of dust these parameters become important. This view was corroborated by Rivera-Thorsen et al. (2015) who studied the outflow properties of the Lyman Alpha Reference Sample (LARS) and found that neutral gas outflow velocity, as traced by absorption lines of low ionization state elements (so called LIS lines), did show a correlation with the escape of Lyα. However, as seems to be usual in Lyα studies, there were galaxies that went against this trend. Henry et al. (2015) studied $f_{esc}^{Ly\alpha}$ correlations in a sample of Green Pea galaxies and found that $f_{esc}^{Ly\alpha}$ strongly anticorrelates with the Lyα peak separation which primarily encodes column density. From their correlations they conclude that column density effects dominate over kinematics in their sample.

There have been a variety of different correlations or potential correlations suggested between Lyα and parameters as more data have become available. For instance the ratio of doubly to singly ionized oxygen emission lines ([OIII] over [OII]) has garnered some interest. The physical process behind this is that having high [OIII]/[OII] could indicate that the ISM of a galaxy is highly ionized and may indicate that this ionized medium is not surrounded by any significant neutral medium, often referred to as a density-bounded HII region. If there is a lack of dense neutral medium around the ionized region then Lyα

should be able to escape from the galaxy relatively easily (Jaskot and Oey, 2013). Such conditions would favor the escape of Lyman Continuum (LyC), i.e. ionizing radiation, as well as Lyα, and some observations do seem to bear this out (Izotov et al., 2016, 2018), which has lead to a great deal of interest in the [OIII]/[OII] diagnostic. However, Izotov et al. (2020), showed that in a sample of eight galaxies selected specifically to have high [OIII]/[OII] only five show strong Lyα emission (EW > 20Å) while the remaining show weak emission (EW $4-7$Å) superimposed on absorption, again demonstrating that high [OIII]/[OII] is not a sufficient condition for predicting Lyα. Similarly Izotov et al. (2021) show that LyC emission appears to only weakly correlate with the [OIII]/[OII] ratio. This work was significantly expanded by the Low z Lyman Continuum Survey (LzLCS Flury et al., 2022a,b). Flury et al. (2022b) found that [OIII]/[OII] ratio does show a significant—but weak— correlation with the LyC emission in a significantly larger sample of galaxies. Clearly quantities parametrizing ionization, such as [OIII]/[OII], are interesting for the study of both Lyα and LyC escape but they do not seem to be sufficient to fully explain them. We look closer at such ionization measures in **Paper V** (see Chapter 6.5).

There have been other methods proposed for determining how much of the emitting ionized region is covered by neutral gas. Rivera-Thorsen et al. (2015) used LIS lines to trace the neutral gas column and determine a covering fraction of HI in the LARS galaxies. While they find that this parameter correlates with $f_{esc}^{Ly\alpha}$, they again note that there are galaxies in the sample with both low neutral gas covering and high outflow velocities that have very low escape of Lyα. They therefore conclude that no single effect alone controls the escape of Lyα. The same conclusion was also reached by Hayes et al. (2014) who looked at correlations between Lyα and several other galaxy parameters for the 14 original LARS galaxies and found that there are indeed correlations with e.g. dust, star-formation rate, stellar mass etc but that all of these show significant scatter even with just 14 galaxies.

4.1 Bringing it together—Multivariate Lyα studies

As we have seen the general conclusion from the many studies that have looked for parameters controlling Lyα luminosity or escape fraction has been that,

while correlations are indeed present, assigning dominant roles or orders of precedence is difficult and there is always significant scatter in the relations. This difficulty in predicting Lyα has recently sparked some interest in whether multiple variables could be brought together to predict Lyα to greater accuracy than any single correlation.

One of the earliest examples of multivariate Lyα prediction was Yang et al. (2017) who used HST *Cosmic Origins Spectrograph* (COS) observations of low redshift galaxies to try to build a predictive model for the escape fraction of Lyα based upon the dust content and the kinematics of the observed Lyα spectra. Specifically they used dust extinction (E(B-V)) estimated from Hα and Hβ and the velocity offset of the red Lyα peak. The red peak velocity is assumed to be an indicator of the amount of neutral hydrogen present in the system since a higher column density of HI would mean that Lyα needs to shift further from the resonance frequency to be able to escape, and therefore the peak would be located further from line center.

They then fit a relation of the form

$$\log(f_{\rm esc}) = a \times (\mathrm{E(B-V)})/0.1 + b \times v_{\rm red}/100 + c.$$

The relation performed quite well across their sample of galaxies but nevertheless has an intrinsic dispersion of around 0.3 dex on a variable with a dynamic range of only ~ 2 dex. Their relation is shown in Figure 4.2a.

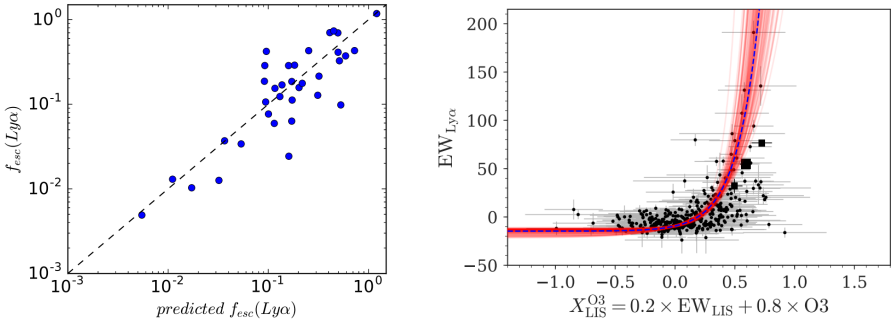

(a) Prediction from Yang et al. (2017)

(b) Prediction from Trainor et al. (2019)

Figure 4.2: Two multivariate predictive relations for Lyα related quantities. Panel *a)* shows the relation from Yang et al. (2017) predicting the escape fraction of Lyα whereas Panel *b)* shows the result of Trainor et al. (2019), predicting the EW of high redshift Lyα emitters.

Trainor et al. (2019) also attempted to derive a predictive relation for the Lyα EW using a large quantity of Keck data of high redshift Lyman α Emitters (LAEs). The relation was based on low ionization state (LIS) line EWs, encoding the covering of neutral gas, and the [OIII] over Hβ ratio which encodes the ionization state of the galaxy as well as whether it is likely that the ionized regions of the system have been able to break through the dense neutral ISM. From these physical parameters they construct a single predictor they call $X_{\rm LIS}^{\rm O3} = 0.2 \times {\rm EW}_{\rm LIS} + 0.8 \times \log\left(\frac{\rm OIII\lambda 5008}{\rm H\beta}\right)$. They then fit an exponential function to this quantity to obtain a relation for Lyα EW:

$$\mathrm{EW}_{\mathrm{Ly}\alpha} = -15 + 5 \times e^{X_{\rm LIS}^{\rm O3}/0.19}$$

The exponential fit is shown as the red line in Figure 4.2b. The relation shows a reasonably strong predictive potential although exactly how large the dispersion is is difficult to quantify and comparisons between the two works are non-trivial due to methodological differences between Trainor et al. (2019) and Yang et al. (2017).

The predictive potential of multivariate analysis of Lyα is the core motivation of **Paper I** (Runnholm et al. (2020)). We wanted to see if the information conveyed in each of the multitude of measured quantities we have for the LARS galaxies could be combined into a relation for predicting the main Lyα quantities – luminosity, $\mathrm{f}_{\rm esc}^{\rm Ly\alpha}$ and EW. Specifically we wanted to see if it was possible to do this without deliberately choosing which variables should be included in the fit, in contrast to the works of Yang et al. (2017) and Trainor et al. (2019).

The LARS galaxies were selected to be highly star forming based on their far UV luminosity: $9.5 \leq \log(\nu L_\nu / L_\odot) \leq 10.7$ and their Hα equivalent width (EW$>$ 100Å) in order to make sure that Lyα photons were produced in these systems. The sample was later extended with a further 28 galaxies for which the selection criteria were relaxed to Hα EW $>$ 30 Å. All 42 galaxies lie between redshift 0.028 and 0.181, and the low redshifts of the targets mean that their internal properties and the impact on Lyα emission can be studied in detail. The LARS project has also gathered a very large amount of ancillary data, including UV spectroscopy, optical spectroscopy and HI observations giving us many variiables to use in a multivariate prediction.

There are many ways of bringing information from multiple variables together into a predictive relation, and an infinite amount of functional forms such a relation can take. However, we only have a finite amount of data to work with; in the case of **Paper I** we had the 42 LARS and eLARS galaxies. One therefore has to pay close attention to the choice of functional form and specifically to the number of free parameters. In order to keep the number of free parameters as low as possible, we limited the fitting function to a simple linear form. A traditional linear regression also has the advantage of very easily generalizing into multiple dimensions, allowing us to incorporate many variables into the fit.

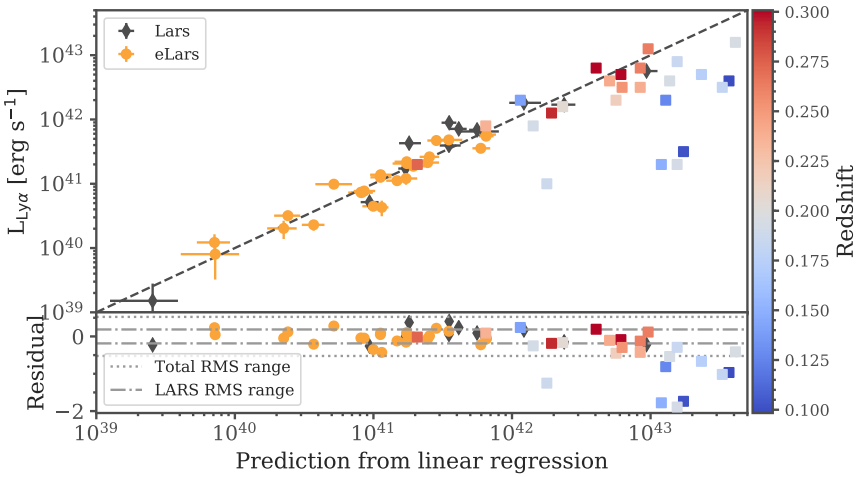

Figure 4.3: Figure from **Paper I**. Predicted versus observed Lyα luminosity for LARS (black) and eLARS(orange) samples. Reference sample from Yang et al. (2017) (not included in the fit) is shown as square points and redshift of the points indicated by the color.

In machine learning, and when building predictive relations in general, it is very important to somehow normalize variables. i.e. to make sure that the scale of each variable is comparable to the others included. If this is not the case it is possible that variables are given higher weight in the fit just because their scale is intrinsically higher (such as a luminosity ($\sim 10^{42}$) compared to a gas velocity ($\sim 10^{2}$)) even though the predictive power of that variable may be smaller. To prevent this in our case we applied a log scaling to the data which compresses the space and makes the numbers much more comparable.

Additionally, it is important to note that this transforms the linear regression to a power law regression.

In **Paper I** we used the LARS and eLARS datasets which covers quite an extensive range of measurements to construct several multivariate regression models for predicting Lyα luminosity, EW and $f_{esc}^{Ly\alpha}$. In order to achieve some separation of concerns and applicability we split the data set into derived variables, and pure observables. We found that it is possible to predict the Lyα luminosity quite well, reaching dispersions as low as 0.19 dex while spanning a full 4 dex in dynamic range, but that second order quantities, i.e. EW and $f_{esc}^{Ly\alpha}$ are significantly more difficult to predict.

Box 4.2: Forward and backward variable selection

The principle behind forward selection is to fit a predictive model on each of the variables we want to include separately and see which single variable model performs best. This variable is then selected as the most important. Next, one fits this first selection together with each of the other variables and the variable that adds the most performance to the model is selected as the second best. The process is repeated for all variables to create a full ranking.

Backward selection is very similar except it starts from the full model and sequentially removes the variable which adds the least to the model until only one variable remains.

However, in order for a relation such as this to be useful it needs to perform well on galaxies that were not included in the model fitting process, something which neither Yang et al. (2017) nor Trainor et al. (2019) tested. The primary reason for not testing a derived relation outside of the sample it was derived upon, is a lack of comparable and separate data. As we saw in previous sections, small datasets have been an issue for the field of Lyα emission research for a long time and having the "luxury" of a set of separate but comparable data is therefore rare. For the work in **Paper I** we were fortunate that the sample of Yang et al. (2017) in fact contained most of the variables we used from the LARS data and we were able to measure the remaining parameters from the publicly available SDSS spectra. Therefore we could test how well our relation would generalize to other samples. The result of this experiment is shown,

together with the prediction of our original LARS galaxies in Figure 4.3. We can see that the prediction performs quite well both for LARS galaxies and the additional reference sample. We also note that the performance on the reference sample seems to get worse at lower redshifts. This is most likely due to the fact that the Lyα luminosities of those galaxies were observed with COS which has a relatively small 2.5 arcsecond aperture. This means that objects that are more nearby are likely to have angular sizes larger than the aperture, especially in Lyα and that these measurements therefore do not capture the full Lyα flux.

We can also look more closely into the variables that are included in this relation, and quantify how much they each add to the prediction. This process is known as variable selection (see Box 4.2) and lets us quantify which variables are the most important for the prediction. We found that the most important observable by far is the FUV luminosity and that the second most important is the size of the galaxy measured from the FUV image. The interpretation of this is that the FUV luminosity correlates with Lyα production, since it is a star-formation rate indicator, and also with the dust absorption at wavelengths close to Lyα. That size comes into it is most likely due to the fact that a more compact star forming region more easily creates outflows (Heckman et al., 2011) and potentially also ionized channels, both of which help Lyα escape.

The methodology that we developed for **Paper I** is also further used in **Paper V** where we looked into the possibility of using multivariate analysis to predict Lyα spectral properties as a complement to the analysis I have presented here. I will discuss the results of **Paper V** in much more detail in Chapter 6.5

5. Spatially resolved Lyα observations

Paper I demonstrated that the total Lyα luminosity can be accurately predicted by using a combination of many other variables. Some of the variables that proved to be important were related to the radiative transfer effects, such as gas kinematics for example, but that analysis did not allow us to quantify how important radiative transfer effects really are for Lyα. In Chapter 3 I discussed resonant scattering and radiative transfer and what the impacts of these processes may be on Lyα. Specifically I noted the random walk that Lyα has to make before escaping a system. While it is theoretically clear that this has to happen for Lyα to escape galaxies that have any substantial HI in their ISM, it is not clear at what spatial scale this scattering happens. Does the Lyα transfer far enough out of the core wavelength already inside the ionized region around the massive stars due to the small fraction of residual neutral hydrogen, or does it scatter further out before having a big enough frequency excursion to escape?

While the spatial and spectral scattering are intimately linked in the physics, they require very different observations to study and therefore I have elected to discuss them separately. In this chapter I focus on the spatial scattering of Lyα and discuss observations trying to quantify how important scattering effects really appear to be in real galaxies. I will discuss the effects of transfer on the spectral dimension in Chapter 6.

5.1 High prevalence of Lyα halos at high-z

At sufficiently high redshifts ($z \gtrsim 1.5$) Lyα enters the optical wavelength range which means that it becomes readily observable with large ground based telescopes. This, together with the fact that a large fraction of all the ionizing radiation in a galaxy gets reprocessed into Lyα, means that it is potentially

a very bright beacon of star-forming galaxies in the high-z universe. Ground based observations also make it relatively easy to conduct large area surveys which can then detect substantial numbers of Lyα emitting galaxies. Many studies of Lyα have therefore naturally focused on high redshift observations. Among the earliest examples is Hu and McMahon (1996) who used narrow-band imaging (see box 5.1) to detect 2 Lyα emitters at redshift 4.55. In the years following this the number of detections increased and high redshift Lyα emitter samples grew significantly.

Box 5.1: Narrowband Lyα detection

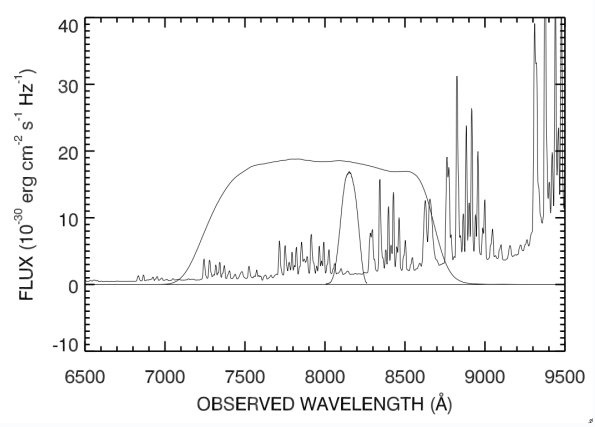

The basic technique behind narrowband emission line searches is quite straightforward. The field is observed using a narrowband filter, i.e. a filter only spanning some tens of Å, and the same field is also observed using using at least one broad band filter that covers the same wavelength range. One can then measure which galaxies have a significant excess of flux in the narrowband filter compared to what would be expected based on the continuum estimate from the broadband filter. Such an excess indicates the presence of an emission line in the narrowband filter. The most basic filter setup is illustrated in the figure which is from Hu et al. (2004). However, in order to exclude low-z interlopers, such as strong [OIII] emitters, more filters are generally needed.

If the target is to quantify spatial scattering however, observations need to provide two things. The first is that we want to compare the Lyα emission with the stellar component, requiring the stellar continuum to be detected—making

faint Lyα emitters difficult to study. The second is that we are interested in studying how much bigger Lyα is compared to the stars, which means that we need to detect very faint Lyα emission. This last part is particularly problematic at high redshift due to something called cosmological surface brightness dimming (Tolman, 1930, 1934). Essentially this describes how much fainter a surface of a particular angular extent is depending on what redshift you are observing it at. This dimming is a very strong function of redshift—proportional to $(1+z)^4$—meaning that it is very difficult to detect faint extended Lyα emission around high-z galaxies. One way to get around this is to use the fact that you can observe large samples to your advantage by stacking the observed galaxies together. Steidel et al. (2011) did this with a sample of continuum selected Lyman Break Galaxies (LBGs) observed with narrowbands and they found, not only significant Lyα emission, but that it seems *very* extended compared to the stellar components. The stacks of the UV light and the Lyα are shown in Figure 5.1 and very clearly shows the UV emission to be much more compact than the Lyα.

They fit the Lyα halos using a declining exponential of the form

$$SB(r) = Ae^{\frac{-r}{r_{sc}}}$$

where SB is the surface brightness at a given radius r, A is the amplitude and r_{sc} is the scale length, i.e. how fast the function declines with radius. Similar models have been used in many subsequent works. They found halo scale lengths around 25 kpc, compared to the 3.3 kpc of the UV emission. It was clear from this that the galaxies had a strong halo of Lyα emission.

Since this result there have been may studies looking at Lyα halos and trying to determine their prevalence around high-z galaxies. While Steidel et al. (2011) studied bright continuum selected galaxies, Feldmeier et al. (2013) used emission line selected LAEs, i.e. galaxies that are intrinsically much fainter. They found very little evidence of Lyα halo emission in most of their stacks but on one substack they found halos with a 3.3 kpc scale length—much smaller than that found by Steidel et al. (2011). Matsuda et al. (2012) studied a large sample of more than 2000 LAEs and found that they did show halo emission in the stacks and they explained the very large scale lengths of Steidel et al. (2011) as a result of looking at bright galaxies in clustered environments,

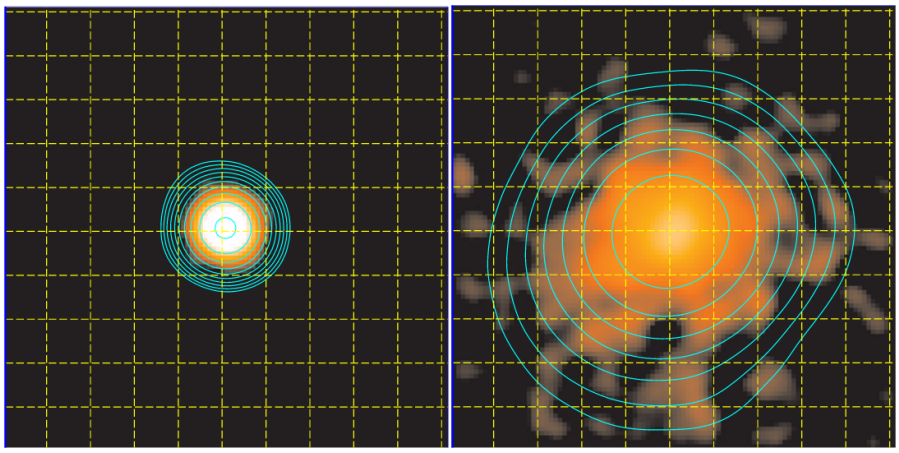

Figure 5.1: Left panel shows the stack of UV emission of LBGs from Steidel et al. (2011) and the right shows the corresponding Lyα stack. Lyα is clearly far more extended than the stellar emission.

and that such halos were less representative of galaxies in the field.

Momose et al. (2014) used a very large sample of several thousand LAEs ranging from redshift 2.2 to 6.6 observed with the Subaru Suprime Cam instrument to characterize Lyα halos, again using stacking analysis. They found that these Lyα selected galaxies appeared to have typical scale lengths around 5-10 kpc. They also were able to determine that there was no sign that these scale lengths changed across the redshift range they were studying. It is worth noting that the difference in cosmological surface brightness between redshift 2.2 and 6.6 is a factor of 32, which corresponds to a factor of 1000 in observing time to reach the same surface brightness sensitivity. However, despite this complication, the non-evolution remains interesting in itself since it implies that the properties of Lyα halos would be constant despite the very large changes in the general structure of the galaxy population and the universe as a whole that has happened during that time.

From all of these results it seemed then that Lyα halos were commonplace around high redshift galaxies. However, because the analysis was done on stacked samples, i.e. averages, exactly how common could not be determined, nor could the magnitude of the variance between galaxies.

This changed with the introduction of a new type of instrument—high sensitivity, large field of view integral field spectrographs (IFSs). These instruments use advanced optics to record a spectrum for each pixel in the image.

This makes them very suited for searching for line emitters such as LAEs. The two prime examples of such instruments used for Lyα halos are the Multi Unit Spectroscopic Explorer (MUSE) (Bacon et al., 2010) on the Very Large Telescope, and the Keck Cosmic Webb Images (KCWI) (Morrissey et al., 2018). Wisotzki et al. (2016) used MUSE to detect individual halos around 45 galaxies at redshift 3–6. They found that individual halos had scale-lengths between 1 and 5 kpc, which is notably smaller than 25 kpc scale lengths of the halos in Steidel et al. (2011). However, importantly, they find that the halo scale lengths are 10 to 15 times larger than the UV continuum. This study was significantly extended by Leclercq et al. (2017) who used the full MUSE-Wide and MUSE-Deep surveys to study the individual halos around 145 LAEs. They confirmed the results of Wisotzki et al. (2016) that Lyα appears to be around 10 times the size of the UV emission measured from HST imaging. They also confirmed that there appears to be no significant evolution across the redshift range between 3 and 6.

5.2 Halos in the low-z universe

As we have seen, high-z observations are very well suited for observing large samples of Lyα emitting galaxies and recent work has unequivocally showed that Lyα halos are a commonplace, if not ubiquitous, feature of star-forming galaxies at high-z. However, there are a number of questions that are very difficult to answer with high-z observations. One strong limitation is the lack of spatial resolution, which means that small scale structural differences between Lyα and stars and the complex interplay that happens inside the ISM is virtually impossible to study. A second limitation is that ancillary information such as Hα has not been observable at these high redshifts. This means that while Lyα halos are readily detectable, their source cannot be quantified. Essentially, without the addition of deeper UV and Hα data we cannot attempt to tell exactly what process causes Lyα halos to form—for instance the halo could be produced entirely in situ or be composed of all scattered radiation or any combination of such processes. Beginning to answer this is one of the main points of study of **Paper II** and we will discuss it more in Chapter 5.2.2.

5.2.1 LARS

To study Lyα halos at low-z we need to obtain images of the emission line but unfortunately this is far from trivial. One of the primary difficulties comes from the UV wavelength of Lyα; since the atmosphere absorbs UV light, this limits us to using space based observations. That is not the end of atmosphere related issues unfortunately. The Earth's atmosphere also emits strong Lyα radiation, which is very problematic for Lyα observations (see Box 5.2). Additionally, neutral hydrogen in the Milky Way leaves a strong broad absorption imprint on spectra. Observations are therefore limited to galaxies with recession velocities large enough that their Lyα is clearly separated from the geocoronal emission and Milky Way features. This corresponds to something like $\gtrsim 2500\text{kms}^{-1}$.

Box 5.2: Milky Way and Atmospheric Lyα

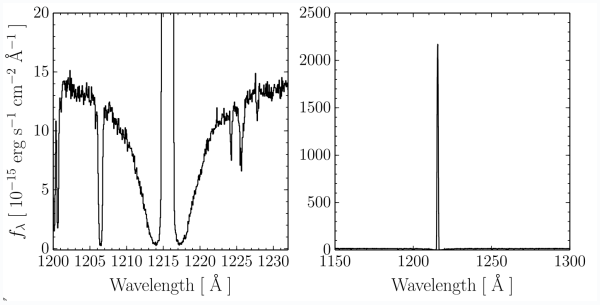

Figure from Hayes (2019). Left panel spectrum shows a spectrum of a BL Lacertae object which is quite flat and featureless (Hayes, 2019) with the clear Milky Way absorption feature and the strong geocoronal Lyα line superimposed. The right panel shows a zoomed out version of the same spectrum to illustrate the relative strength of the geocoronal emission.

Moreover, the throughput of detectors in this wavelength range is in general quite poor. For example, early detectors on the HST that included Lyα filters had throughputs of less than 0.3% (Östlin et al., 2014). When the Advanced Camera for Surveys (ACS) Solar Blind Channel (SBC) was installed on HST it became possible to tackle this issue. Hayes et al (Hayes et al., 2009; Östlin et al., 2014) developed a technique that uses adjacent broadband (long-pass) filters on the ACS camera on HST to synthesize an effective narrowband

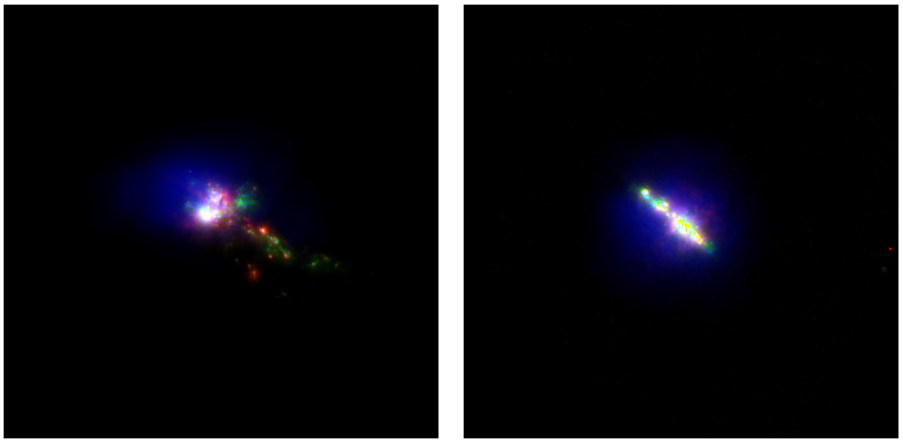

(a) LARS 01 **(b)** LARS 05

Figure 5.2: Lyα imaging of two galaxies in the LARS/eLARS project. Blue encodes Lyα, red Hα green far UV emission. It can be seen in both of the panels that the Lyα emission appears more extended than the central star-forming regions and specifically it appears to be more extended than Hα in these images, which could be indicative that Lyα undergoes spatial scattering.

with significantly higher throughput of Lyα than could be achieved with other cameras and filters on the HST. One of the major issues with this observational technique is that there is significant contribution from the continuum around Lyα that needs to be subtracted. Since the synthesized narrowband is not as narrow as conventional narrowbands (Hayes, 2019), and the continuum level varies rapidly in this region of the spectrum, accurate modelling of the continuum is needed. This requires modelling the stellar population of the galaxy and estimating the continuum level from the models which requires sufficient additional observations in other wavelength bands for a good fit to the spectral energy distribution (SED) to be obtainable.

This method was applied to obtain Lyα imaging for 14 galaxies in the LARS sample (Östlin et al., 2014) and later extended with a further 28 galaxies in the eLARS sample. Examples of Lyα imaging of two galaxies from these samples are shown in Figure 5.2. What can be clearly seen from this figure is that, while the FUV (green) and Hα are quite concentrated to the star-forming knots, the Lyα (blue) shows a much more spread out 'fuzzy' structure. This pattern is repeated throughout the LARS sample. Lyα and Hα are produced by the same radiative recombination cascades so we would expect the emission to

be co-localized. The fact that it is not, could be indicative of significant spatial Lyα scattering in these systems. However, it should be kept in mind that Hα is expected to be $\sim$ 10 times fainter than Lyα based on standard recombination theory which means that very deep Hα observations are required to firmly conclude that Lyα is spatially scattering and not being produced where we see it in these images.

Hayes et al. (2014) studied the spatial extent of Lyα in the LARS sample and found typical sizes around 1 to 4 times that of the UV. Further study of the spatial profiles of LARS and eLARS was done by Rasekh et al. (2021) who found a larger spread of Lyα to UV sizes more akin to the values found at high redshift. Rasekh et al. (2021) also found that the centroids of the UV and Lyα emission are significantly offset from one another—a clear indication that Lyα is not emitted cospatially with the stars. Whether this is due to Lyα scattering away from the production site before escaping to our sightline, or due to Lyα directly escaping from regions of ionized gas displaced from the stars, is not yet clear.

5.2.2 Optimized low surface brightness observations

The LARS project is optimized to study the very smallest scales of Lyα emission and the details of scattering and escape. However, this means that the galaxies are quite big compared to the field of view of the SBC camera. This can potentially cause issues when trying to do subtraction of backgrounds and treating instrumental issues such as dark current. If Lyα is as extended at low-z as it is at high-z there is a significant risk that extended Lyα may be subtracted when the background is estimated. Additionally, the large galaxy sizes mean that characterizing and subtracting the complex dark current patterns in the SBC detector is not possible. While the LARS program was designed to take advantage of the times when the SBC is at its coldest to minimize this issue some dark current signal will still be present in the images. It is not clear to what extent such issues affect the LARS data, and unfortunately there is no apparent way of quantifying any such impact. For **Paper II** we wanted to determine whether the Lyα observations are affected by such issues and to provide a solid anchoring at low redshift for Lyα halo observations. Therefore we designed a HST program that minimizes these uncertainties, targeting 7 galax-

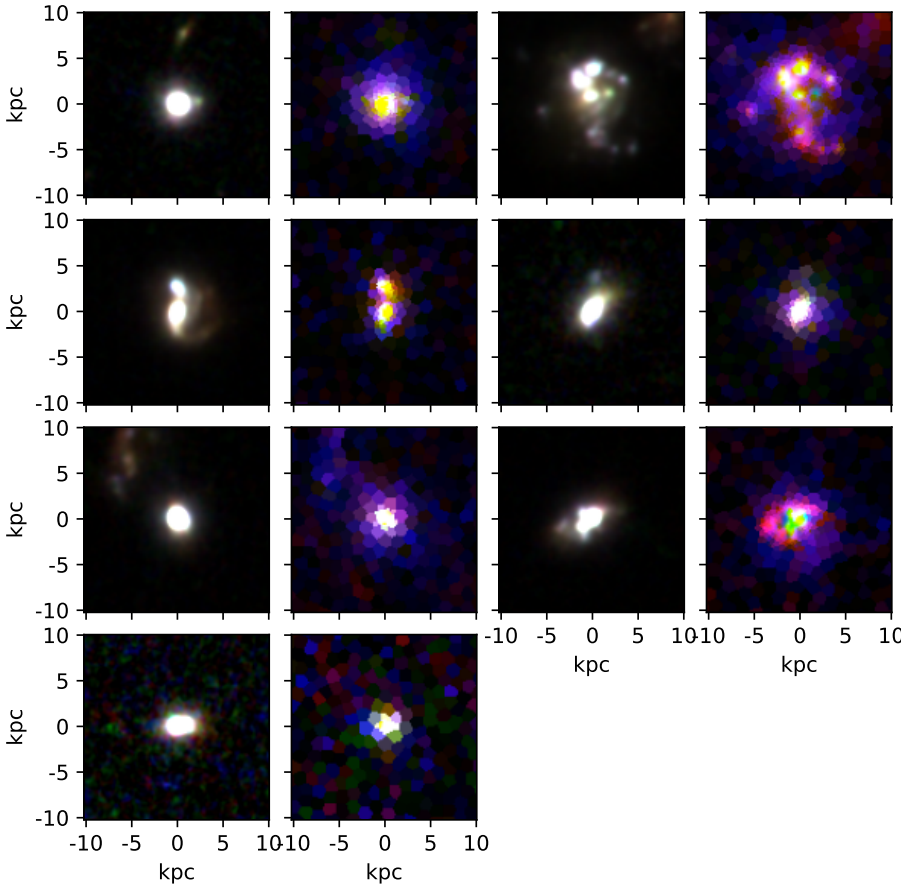

Figure 5.3: Optical and Lyα composite images of the Halos sample of galaxies.

ies at $0.23 \leq z \leq 0.31$. The aim of the program was to see if the non-evolution of Lyα halos that is observed at high-z holds to the present day.

The basic target selection of the program was very similar to that of LARS, focusing on selecting star-forming galaxies (Hα EW > 100Å, and FUV magnitude between -17.5 and -22), that are not significantly extincted by Milky Way dust (foreground reddening less than 0.2 magnitudes). The biggest difference to the LARS selection is in the redshift range which was restricted to between 0.23 and 0.31. This range ensured that Lyα would fall in the correct filter on the SBC camera (F150LP) and not contaminate the adjacent filter that is used for continuum estimation (F165LP), and, additionally, made sure that OI emission from the Earth's atmosphere would not be transmitted by either

filter.

The data processing was done in a manner very similar to the LARS project using the Lyman Alpha eXtraction Software (`LaXs`, Hayes et al., 2014, 2009; Östlin et al., 2014, and Melinder et al, in prep) to do the SED modelling required to estimate the continuum. However, we included additional fitting of the dark current of the SBC detector, which was found to be significant, as well as further background subtraction steps in order to ensure the best possible data quality of the Lyα images. We found Lyα emission around all 7 of our galaxies despite Lyα emission not being part of the selection criteria for the sample and total escape fractions between ~ 0.7 and 37 %. We show optical composites and 3 color composites of Lyα, Hα, and FUV in Figure 5.3. From the optical images it is clear that the galaxies span a range in both morphology and size from very compact and circular objects, to extended multicomponent systems. The Lyα images also show that most galaxies have extended Lyα emission lying outside the apparent UV emission. To improve the signal-to-noise of the elements used in the fitting, we use a Voronoi Tesselation (Diehl and Statler, 2006) to adaptively bin the data which can clearly be seen in the images.

We create profiles of the surface brightness (SB) as a function of radius to properly characterize the Lyα emission. It is common to do this by creating azimuthally averaged bins; however this can lead to issues when fitting the profiles so we instead opt to show the individual Voronoi cells where each cell has been given a radius that is the average distance to the center of its constituent pixels. An example SB profile is shown in Figure 5.5.

We begin the fitting by following the procedure of Leclercq et al. (2017), using 2 exponential components—one core and one halo component:

$$\mathrm{SB}(r) = A_1 e^{-r/r_{\mathrm{core}}^{\mathrm{UV}}} + A_2 e^{-r/r_{\mathrm{halo}}^{\mathrm{Ly}\alpha}}$$

where $r_{\mathrm{core}}^{\mathrm{UV}}$ is the scale length of the central emission and $r_{\mathrm{halo}}^{\mathrm{Ly}\alpha}$ is the scale length of the extended halo emission. Again, following Leclercq et al. (2017), we fit $r_{\mathrm{halo}}^{\mathrm{Ly}\alpha}$ on the FUV emission, based on the assumption that the central Lyα should roughly follow the stellar content of the galaxy. Using this procedure we get results that we can directly compare with high-z, and the comparison is shown in Figure 5.4. We use the superscript to denote what data the scale

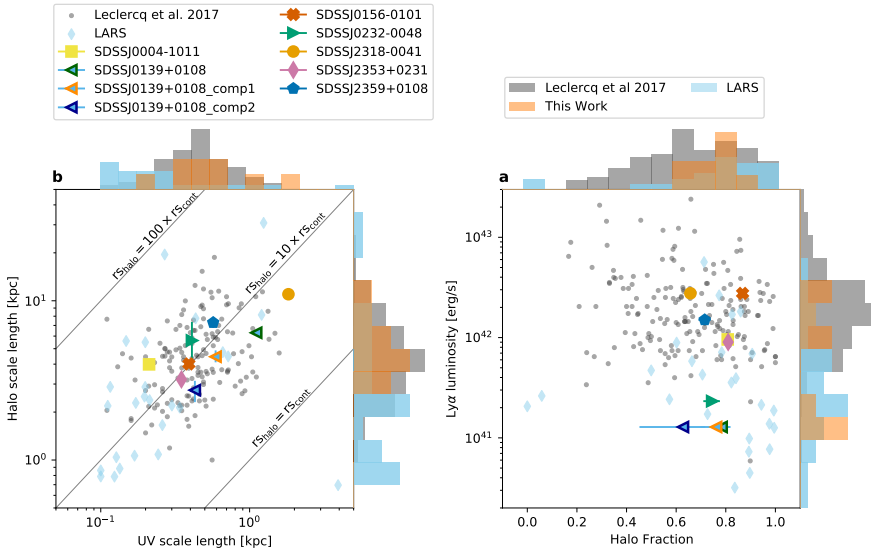

Figure 5.4: Figure from **Paper II**. Left panel shows the scale length comparison between high-z and the halos and refitted LARS results and the right panel shows a comparison of the fraction of flux in the halo component.

length was fitted on.

From this comparison it is quite clear that the results from **Paper II** are entirely consistent with high-z results. This shows that Lyα halos appear to be the same from redshift 6 to redshift ~ 0—a span of over 13 billion years.

However, working at low redshift translates to much less surface brightness dimming compared to high-z. We can therefore detect faint UV emission and we find that the FUV surface brightness profile is not particularly well described by a single exponential function. The right panel of Figure 5.5 shows quite clearly that the green points appear to have a secondary flatter component that deviates from the core exponential. We therefore introduced a new model:

$$\mathrm{SB}(r) = A_{\mathrm{core}}(A_1 e^{-r/r^{\mathrm{UV}}_{\mathrm{core1}}} + A_2 e^{-r/r^{\mathrm{UV}}_{\mathrm{core2}}}) + A_3 e^{-r/r^{\mathrm{Ly}\alpha}_{\mathrm{halo}}}$$

While this may look complicated it is a simple modification of the previous model—we have simply added one component to the core. The two core component scale lengths, $r^{\mathrm{UV}}_{\mathrm{core1}}$ and $r^{\mathrm{UV}}_{\mathrm{core2}}$ are fitted on the FUV emission. This model is illustrated in the left panel of Figure 5.5.

The new model provides a better description of the data in all of our galax-

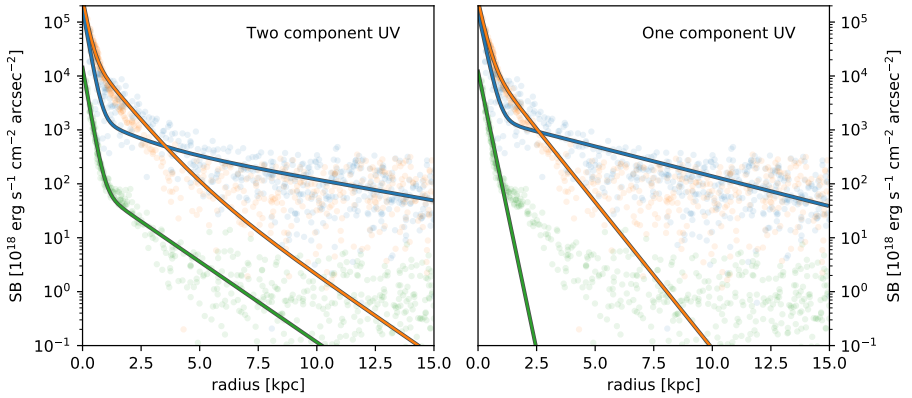

Figure 5.5: Figure from **Paper II**. Points show surface brightness profiles for Lyα, Hα, and FUV. Right panel shows the 2 component model from Leclercq et al. (2017). Left panel shows the new three component model with two components fitted on the FUV and one additional halo component.

ies and also significantly lowers the flux contribution from the halo compared to the two-component model. This has interesting implications for the high-z results we discussed previously. If halo hosting galaxies in general have a faint UV component that high-z observations have been unable to reveal, the importance of Lyα spatial scattering may be lower than previously believed. However, all our galaxies still show significant halo emission even when taking this faint UV into account. The question that then naturally arises is what is the source of the halo Lyα emission?

5.2.3 The Source of Lyα halos

As we noted in the introduction to this Chapter, it is difficult to make strong statements about the origin of Lyα halos at high-z. However, one major advantage exists for such studies—Integral Field Spectrographs. They can show both the spatial and spectral variations of Lyα at the same time which can be used to make some statements about the probable origins of Lyα. For instance Erb et al. (2018), Leclercq et al. (2020) and Chen et al. (2021) were all able to study a combination of the spectral and spatial profiles of Lyα around high redshift galaxies. Erb et al. (2018) only studied a single target but found that the central galaxy was dominated by red peak Lyα emission, and that the blue emission became more important at larger radii. Chen et al. (2021) found that Lyα showed a distinct red peak dominance in averaged spectra of KBSS galax-

ies out to large galactocentric radii. Similarly Leclercq et al. (2020) found that the halo of their six LAEs are dominated by a broad and distinctly redshifted Lyα component. The profiles in all these works are indicative that Lyα has been significantly scattered and that this scattering has happened in a outflowing medium. Based on this both Leclercq et al. (2020) and Chen et al. (2021) interpret their observations as indicative that the halo is dominated by scattered radiation from the central target rather than cooling radiation from inflowing gas.

This tells us that the Lyα emission most likely originated from the central galaxies and scattered in some way in the outflows of those galaxies. However, Lyα scatters in even small amounts of HI gas and the spectral profile is quickly reprocessed into the classical two peak or prominent red peak profiles that Leclercq et al. (2020) and Chen et al. (2021) see, as I shall discuss in more detail in the next chapter. The observations therefore cannot tell us how much of the circumgalactic Lyα is produced roughly where it is observed, and how much has scattered far from the production in the central galaxy. To be able to answer this we need to trace the recombining gas, e.g. by using Hα observations. Currently this means studying low-z galaxies (although this might change now that JWST is launched and operating).

We therefore used our Halos project observations to contrast Lyα with, not only the FUV as we have discussed up until now, but also the Hα. The first thing that became apparent was that the Hα is significantly extended compared to the FUV—similar to the Lyα. This indicates that the ionized gas is more extended than the stellar component and giving a first hint at that the source of the Lyα might be in-situ ionizations. We further investigate this by centering the fits to the Lyα surface brightness profile on the Hα. The idea is that if the Lyα halo is dominated by in situ production a rescaled version of the Hα SB should be a good description of the Lyα SB profile and therefore the contribution of any additional Lyα halo component should be low. We find that the Lyα halo component does significantly decrease in importance when conditioning the core on Hα rather than Lyα again indicating in-situ production of Lyα. However, the fraction of flux coming from the halo component is still significant. All in all we interpret this as evidence that Lyα halos are powerered by a combination of in-situ recombination and spatial scattering. Clearly Lyα halos are complex phenomena with multiple sources that act simultaneously and trying

to assign only one dominant mechanism is overly reductive.

6. Lyα Spectra

As we just noted, the works of Leclercq et al. (2020) and Chen et al. (2021) showed that the Lyα spectral profile can be a powerful tool for determining which processes have affected Lyα emission and also perhaps for probing the environment around galaxies. In this chapter we look closer at Lyα spectra and what we can do with them.

In **Paper I** we connected galaxy properties to the total integrated Lyα observables and in **Paper II** we attempted to determine the origin of Lyα halos using comparisons to Hα and FUV imaging. Papers **III**, **IV** and **V** instead focus on the spectral profiles of Lyα and their connection to Lyα scattering, escape and general galaxy properties.

6.1 The Lyα spectral zoo

As early Lyα spectral observations were made, it became clear that Lyα shows a very large range of different spectral profiles. The Lyα profiles observed now range from damped absorption to combined absorption and emission (P-Cygni) profiles to single and double, or even triple, peak emission lines. We show some examples of Lyα spectra obtained with the COS spectrograph that span a range of these different profiles in Figure 6.1. It is interesting to note that all galaxies in Figure 6.1 are from the LARS and eLARS samples, which means that they all follow essentially the same selection criteria (primarily based on active star-formation, as I discussed in Chapter 4.1), and still span the full gamut of spectral profiles.

There are some common characteristic features however. Comparing Lyα emission to non-resonant emission lines such as Hα the first notable thing is the lack of single Lyα peaks centered on the systemic velocity and it is in fact quite uncommon to see any significant flux at the Lyα central wavelength at all. As we saw in Chapter 3 this is because of the very high optical depth

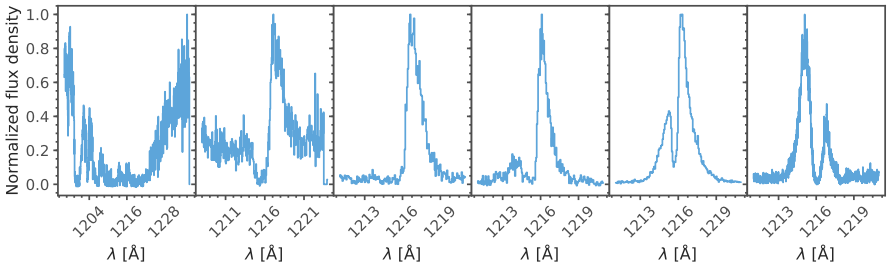

Figure 6.1: Examples of Lyα spectra observed with the COS to illustrate the range of possible Lyα profiles ranging from complete damped absorption, P-Cygni profiles to double peaks, and in some cases a blue peak that is stronger than the red peak.

at line center that arises when the Lyα photons have to travel through virtually any HI in the galaxy. The fact that we do not see central Lyα emission gives a strong observational indication indication that Lyα photons can only escape after some frequency redistribution and that direct escape, through ionized channels in the ISM for instance, is rare. This is further supported by the fact that when only one peak is observed it is most often highly asymmetric with a sharp cutoff on the line center side and a long tail on the other side. There are some notable exceptions to the lack of central emission however, such as the Sunburst Arc (Rivera-Thorsen et al., 2019) which shows a triple peak with two peaks showing significant radiative transfer effects and a superimposed central peak that could be due to direct escape. Such triple peaks have also been pointed out as indicators of strong escape of LyC since if there are channels where Lyα can escape without radiative transfer those channels are most likely very transparent for ionizing radiation as well. In fact, the fraction of Lyα flux at line center was used by Naidu et al. (2022) as an indirect predictor of LyC photon escape together with the separation of the blue and red Lyα peaks.

Another of the most common Lyα spectral characteristics is that the red peak is stronger than the blue peak. This is the spectral pattern that we would expect if Lyα is scattering in a outflowing medium such as a galaxy wind. Such winds are very common in heavily star-forming galaxies (see e.g. Heckman et al., 2011) so finding many red peak dominated Lyα spectra is then expected. However, as usual with Lyα, there are exceptions to this, such as the galaxy

eLARS 07 which is shown in the rightmost panel of Figure 6.1 and has a very prominent blue peak, potentially indicating that this galaxy has a significant inflow of gas.

6.2 Modelling Lyα spectra

Clearly relatively similar galaxies show very different Lyα spectral profiles and it seems that they may carry significant information about the system from which they are emitted. In order to interpret the exact line profiles we need to model them however, and modelling Lyα escape is a complicated problem. Simulating a realistic ISM and Lyα radiative transfer through it from first principles is in general not possible due to the small spatial scales over which it happens. Instead some generalizations have to be made.

One class of generalization that has proven to be highly successful is assuming simplified gas conditions where the geometry is treated as spherically symmetric shells. The highly simplified geometry makes using such models to make any conclusions about how the gas is distributed difficult. However, they are relatively computationally cheap to run and readily interpretable in terms of the kinematics and state of the gas. Therefore several groups have attempted to make inferences about the properties of Lyα emitters based on modelling of their line profiles. Verhamme et al. (2008) used such models to fit the spectra of 11 Lyman Break Galaxies (LBGs) and found that the differences in their spectra were most likely attributable to HI column density and dust variations. While there have been some discussion about how to interpret the result of such simplified models, Gronke et al. (2015) show that the shell models appear reasonably able to recover representative column densities and outflow velocities of the neutral gas. Gronke (2017) studies 237 high redshift galaxies observed with the MUSE integral field spectrograph at the VLT using a shell model. He finds that the spectra can be well fitted with the model and notes that a substantial fraction of the galaxies appear to have quite low HI column densities with $N_{\mathrm{HI}} \sim 10^{17}\mathrm{cm}^{-2}$, which could be part of the explanation of how they are able to emit significant Lyα.

It is quite evident that detailed modelling has the potential to extract useful information from Lyα spectra; however, using full hydrodynamical modelling is too complex to easily apply to the interpretation of large numbers of

observed spectra, and the assumptions going into simpler models complicate the interpretation of the results, especially for simplified models such as shell models (Gronke et al., 2015). Nevertheless, they remain useful tools for guiding interpretations of observations and the investigating average Lyα transfer properties.

6.3 Spectral reference samples and comparisons

As we have seen Lyα spectra show an incredible variety, and how to analyze and interpret them is not straightforward. This has led to many subtly different Lyα analysis methods. An example is how to describe the velocity of the red Lyα peak. This can be done by taking the first moment of the line, finding the wavelength of the peak of emission, or fitting a Gaussian to the line to name a few examples. Similar situations apply to describing things like peak asymmetries or even things like continuum level around the emission line.

While the field has progressed at an incredible rate in the last few years it has nevertheless started to become an issue that many works are difficult to directly compare. This problem also applies to comparisons between observations and theory. The lack of homogeneously analyzed and freely available Lyα spectra makes it difficult to find comparative samples for sanity checks of simulations.

We therefore set out to make a public database where observations of Lyα spectra could be uploaded, and automatically and homogeneously analyzed. The results of this effort is the Lyman Alpha Spectral Database (LASD)[1]. The interface is designed to let users upload Lyα spectra for analysis and to enable simple filtering and downloading of both spectra and derived quantities. At the time of writing the database contains 351 spectra and more than 14000 individual measurements.

The requirement for the analysis to be completely autonomous created some interesting algorithmic challenges—especially when combined with the fact that we needed to be able to process both high and low redshift spectra. Specifically, this meant that we needed to be able to produce a reliable redshift of the galaxy that we can use for analyzing the spectral properties of Lyα, since

[1] `lasd.lyman-alpha.com`

high-z Lyα spectra in general do not have independent redshift confirmations. Unfortunately, this too is made more complicated by resonant scattering since where the Lyα line emission peak occurs with respect to the true systemic redshift depends strongly upon the amount of scattering in the system. If a confirmation of a rough redshift is all that is required, this does not constitute much of a problem. However, if you wish to do kinematics and detailed measurements of the Lyα properties then a more accurate redshift than simply the position of the Lyα peak is required.

One method for deriving redshifts from Lyα lines was developed by Verhamme et al. (2018) who used a sample of 13 LAEs to derive a fitting formula for the systemic redshift with an accuracy, on that small sample, of approximately $100\,\mathrm{km\,s^{-1}}$. In **Paper III** we looked into this issue in more detail and developed a simple, automated algorithm for determining the redshift from Lyα since we expect the Lyman Alpha Spectral Database (LASD) to have to process many spectra for which Lyα is the only detectable line. The algorithm is based on the empirical fact that most Lyα emitters show either 2 peaks or a single red peak that is offset from true systemic redshift. We therefore begin by determining whether there are 2 peaks in the spectrum and if so we place the redshift of the galaxy at the valley, i.e. the minimum between the two. An example of this is shown in the left panel of Figure 6.2. In the case of a single peak spectrum we made the assumption that the peak is located on the red side of systemic redshift. We then find the point where the left edge of the peak reaches the continuum and use that as the redshift estimate. This is illustrated in the right panel of Figure 6.2. It is possible that the peak will be further from the systemic redshift if the column density of hydrogen is high enough. However in that case the scattering has also removed the information from the central part of the spectrum and therefore it will no longer be possible to get a better redshift estimate from the line without modelling.

As a part of **Paper III** we also did a detailed evaluation of the accuracy of this algorithm by applying it to a large number of low redshift galaxies observed with COS where the true redshift could be accurately determined from optical spectra from the SDSS. We found that we were able to determine the redshift to within less than $\pm 200\,\mathrm{km\,s^{-1}}$, even at relatively low spectral resolutions across a large sample of galaxies. Figure 6.3, adapted from that paper illustrates this.

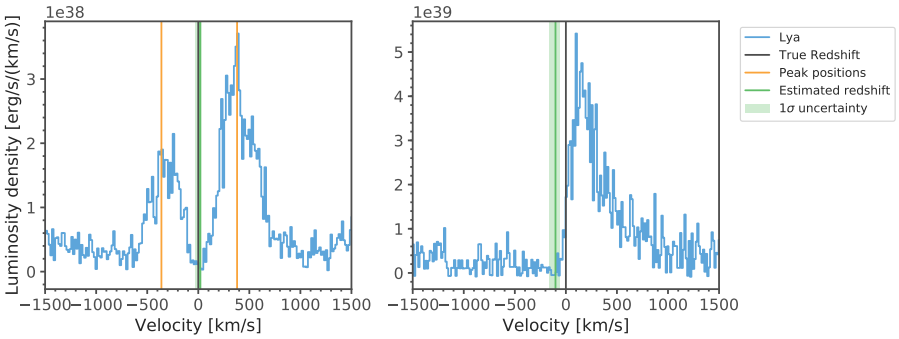

Figure 6.2: Examples of the redshifts determined using the automated algorithm in the Lyman Alpha Spectral Database. Left panel: Redshift determined using the double peak valley detection algorithm. Right panel: redshift determined using the single peak walking algorithm. Both spectra are put into velocities using the true, independent redshift from optical lines—i.e. 0 velocity corresponds to the systemic redshift of the galaxy.

6.4 Evolution of Lyα spectra

The samples in LASD are useful not only for providing comparisons for other work but the homogeneously analyzed spectra can be used for very interesting science in their own right. One particular unique aspect of this sample is that it readily provides Lyα spectra across a very large redshift baseline from redshift ~ 0 to > 6.5. This means that we can potentially use them to study evolutionary trends in Lyα spectra across a large fraction of the age of the universe. This was the experiment that we performed in **Paper IV**. However, the signal to noise of individual LAEs, especially at high-z, is most often insufficient for detailed analysis—such as the detection of weak blue peak emission. Therefore we binned the spectra in different redshift bins to create average spectra with much higher signal to noise ratios.

Several interesting trends became evident when we did this but the primary finding is that the contribution of emission on the blue side of Lyα decreased monotonically with redshift. This is quite clearly visible in Figure 6.4, in particular in the right panel. The question that arises then is why this happens—is it because the LAEs change, or is it the change in the medium in which these galaxies reside? We know that the galaxy population changes across this time span with higher redshift galaxies being, on average, much more extreme in their star-formation than galaxies observed in the local universe. But we also

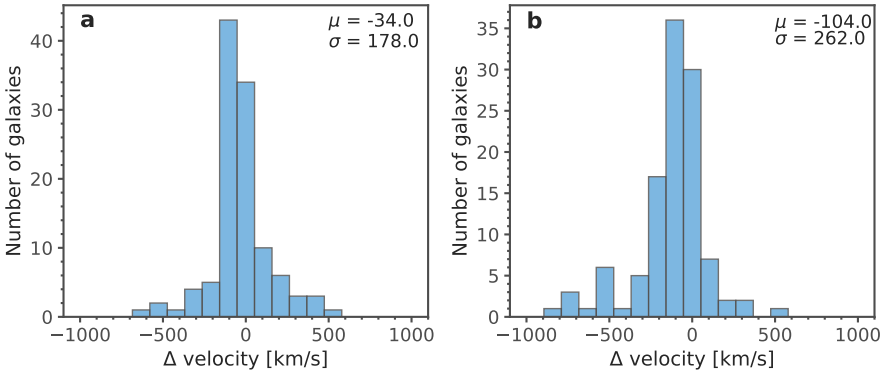

Figure 6.3: Panel a: Distribution of differences between the redshift estimate from the LASD algorithm and the true redshift for 113 COS spectra. Panel b: As panel a but estimated for 113 spectra where the spectral resolution has been significantly reduced (to R$\sim$ 4800) to simulate observation with lower resolution spectrographs such as MUSE. Adapted from **Paper III**.

know that the neutral content of the IGM increases as we look further back in time (Inoue et al., 2014) and Lyα is, as we have seen, sensitive to the neutral hydrogen column.

We therefore set out to determine which of these effects is at play here. The core strategy was to compare the decrease in the blue component of Lyα to that which would be expected by the IGM at the various redshifts. In order to do this we need a reference spectrum that is not affected by IGM absorption that we can use as a comparison. We have a very deep stack of redshift 0 spectra observed with HST where IGM absorption is completely negligible that we can use for this purpose. The second thing we need is a set of measurements of the average IGM HI density as a function of redshift. Fortunately, Inoue et al. (2014) published exactly this based on Lyα absorption in quasar spectra. We then used this prescription and attenuated the COS spectrum by the IGM transmission for each of our redshift bins and compared this with the actual observed Lyα spectrum for that bin. The results of this exercise are shown in Figure 6.5.

The upper panels of Figure 6.5 shows the unattenuated COS spectrum in pink normalized to a maximum of 1 together with the IGM transmission in beige for each redshift bin. The bottom row shows the attenuated COS spectrum plotted over the observed high-z spectrum observed with MUSE. This

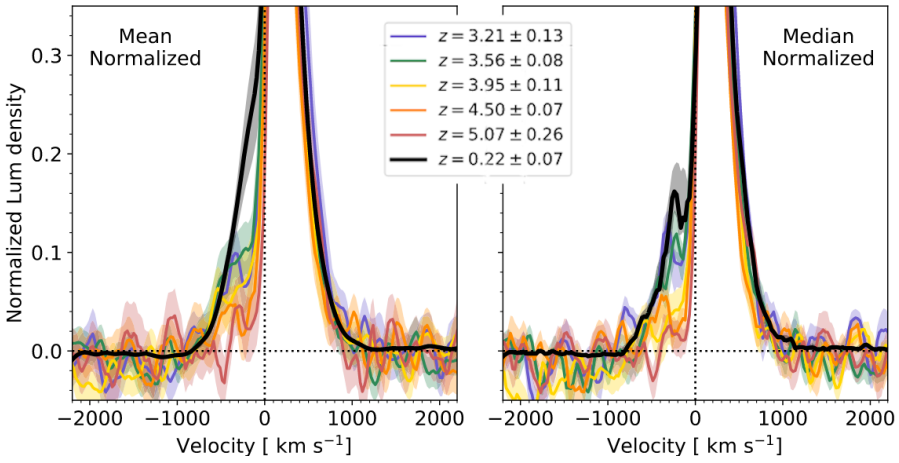

Figure 6.4: Figure adapted from **Paper IV**. Left panel shows the mean on the redshift binned stacks and the right panel shows the median.

row clearly shows that the attenuated COS spectrum agrees very well with the actual observed spectrum for a given redshift bin. From this we can conclude a couple of things: that the Lyα spectra appear to be consistent with having the same intrinsic emitted spectrum across the whole redshift range, and that there is no need for any attenuation variation from LAEs residing in particularly dense or tenuous environments.

So when studying Lyα spectral shapes we found that they appear to be the same across redshifts 0 to 6.6. And when we looked at the spatial extent we likewise found that low redshift Lyα emitting galaxies appear similar to Lyα emitting galaxies at high-z. It is therefore tempting to conclude that this type of galaxy, or at the very least their Lyα emission does not change significantly across the 10 billion years between redshift 0.2 and 6.6. While this conclusion may be too strong, our results nevertheless make it very clear that we can safely try to use detailed low-z results to try to understand high-z LAEs.

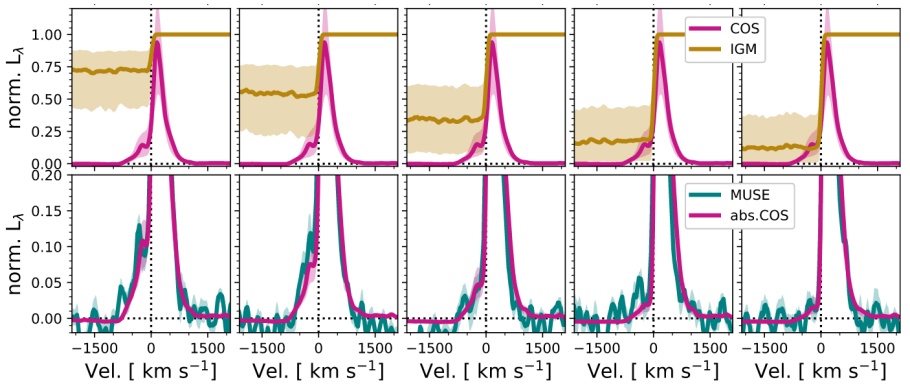

Figure 6.5: Figure from **Paper IV**. Shows an average low-z spectrum attenuated by the IGM at a given redshift compared to the actual observed spectrum at the given redshift.

6.5 Influence of the stars and nebular gas on emitted Lyα

Paper II and **Paper IV** showed that Lyα properties appear to remain relatively constant across a large fraction of the age of the universe. The hope then is that the detailed relationships between the properties of the galaxy and emitted Lyα that we can derive at low-z will hold at high-z and can inform us about the processes occurring in those early galaxies. As we saw in **Paper I** there are some strong relationships between the UV and star-formation properties of the LARS galaxies and their total Lyα output. However, in that work we did not consider the Lyα spectral distributions. In **Paper V** however, we wanted to look more closely at that.

Specifically we looked not only at total Lyα but also at the strengths of emission on the blue and red side of the line as well as the ratio between them. These quantities are important to understand since the spectral distribution of Lyα has strong effects for how it transfers through HI gas, as we saw in Chapter 3. If we want to use observations of Lyα to get measurements of the neutral fraction in the IGM we need to know what the intrinsic spectral profile emitted from the ISM and CGM is. Empirically calibrated relations for the blue and red components of Lyα can help constrain inference about the IGM neutral fraction that relies on assumptions on the intrinsic Lyα spectra of galaxies—such as that of Mason et al. (2018).

We therefore again used the spectral sample of COS observations assem-

bled in the LASD and carefully fitted the optical spectra from the SDSS to derive detailed optical line properties. Additionally, we fitted the stellar spectrum of the galaxies, simultaneously in both the UV and optical range, to obtain in depth information about the underlying stellar population. We then looked for correlations between Lyα and many different stellar and optical diagnostics that can tell us more about the evolutionary state of the galaxy and the state of the nebular gas.

Our primary conclusions from this were:

Ionization state The ionization state of the gas correlates extremely well with Lyα—both red and blue luminosities and equivalent width. The ionization state is often parametrized by the [OIII]/[OII] ratio but we find that line ratios sensitive to even higher ionization states such as [NeIII]/[OII] also show strong correlations with Lyα. This suggests that galaxies with intense radiation fields able to ionize the interstellar gas to very high ionization stages have an environment that is more conducive to Lyα escape.

Stellar evolutionary stage The stellar evolutionary stage, i.e. how old the stellar population is in the galaxy. In this case this was measured both by the equivalent width of Hβ and the age of the modelled stellar population. A younger and more intense stellar population—which has a high Hβ EW—allows more Lyα to be produced and perhaps, through mechanisms like that indicated in the previous point, allows it to escape.

Dust We find that dust, as measured from the Hα/Hβ ratio correlates strongly with Lyα. This is expected since dust absorption is the primary destruction mechanism of Lyα photons as we saw in Chapter 4.

Nebular abundance The metallicity of the gas also shows strong anti-correlations with the emitted Lyα. The mechanism behind this is not completely clear but it may be related to the fact that the metallicity of the gas has an impact on the amount of dust present. Simplistically more metals means more dust and more absorption. However, the gas metallicity also correlates with the metallicity of the stars, which we show in Figure 5 of **Paper V**, and lower metallicity stars emit have harder spectra

with more ionizing photons (Leitherer et al., 1999). Similar strong anti-correlations between Lyα EW and metallicity have also been found by other studies, such as the VANDELS collaboration (Cullen et al., 2020) where they studied a sample of 768 Lyα emitters at redshift 3 to 5.

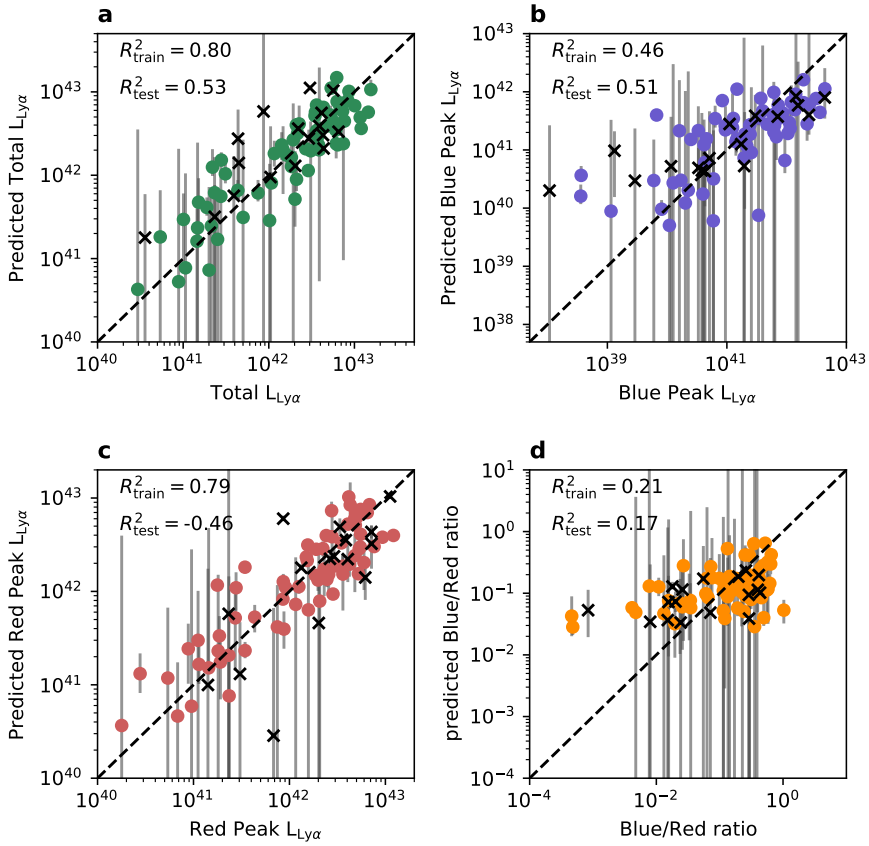

Figure 6.6: Figure adapted from **Paper V**. Panels show the predicted quantity on the y axis and the measured true quantity on x. Panel **a**: Total Lyα luminosity, Panel **b**: blue peak luminosity, Panel **c**: red peak luminosity, and Panel **d**: Blue over Red ratio Colored points indicate the training sample and black crosses indicate test samples.

After this analysis we want to extend the multivariate analysis that we did in **Paper I** to this data set. We therefore subdivide the predictors—in this case the data derived from the optical spectra—in two sets. One used to predict luminosities and the other to predict EWs. The first set consists of line luminosities which are then further pared down by selecting only lines that had a median

signal to noise ratio above 10 across the sample of 81 galaxies. This line list was then further pared down to avoid including the same information twice, for instance by using the sum of the [OII] doublet rather than the individual lines. We then used this set of lines to predict the luminosities of the total Lyα, and the red and blue components and their ratio separately using a standardization procedure that was very similar to that used in **Paper I**.

Figure 6.6 shows the predictions and clearly demonstrates that we can make reasonable predictions of all three peak luminosities with coefficients of determination ($R^2_{\rm train}$) between ~ 0.5 and 0.8, but that the blue peak is significantly more difficult than the total or red peak. This result is quite expected since blue peaks are rarer and the detections are noisier than for the red or total Lyα. The fact that the ratio is very difficult to predict with R^2 of only around 0.2 is a little bit less expected given the performance of the other two predictors. However, this may be due to what I will term the luminosity effect—where the rough luminosity of the target is relatively easy to get right at an order of magnitude level but when the luminosity is normalized out, i.e. in a ratio, the lower dynamic range variability, which is harder to predict, becomes relatively more important. We saw a similar effect in **Paper I** when we applied our predictions to EWs and escape fractions got significant reductions in predictive power compared to the Lyα luminosity predictions.

We find a similar effect in **Paper V** when we try to predict the EWs. For these models we used a set of predictors that were based on ratios instead of absolute luminosities. The results in Figure 6.7 show that we can explain around 50% of the variance in the EWs—significantly lower than for the luminosities but nevertheless a reasonable prediction. However, in the figure the R^2 for the test set is also given. This is a measure of how well the model performs on objects that were not included in the training. The $R^2_{\rm test}$ is considerably lower than $R^2_{\rm train}$ which indicates that we may be slightly overfitting the relation. However, we do find that this quantity is quite sensitive to the exact selection of the test sample.

One way of reducing overfitting is simply to reduce the number of variables included in the fit. But how do we know which variables we should include to make the best possible model? We can use variable selection, which we presented briefly in Chapter 4.1 and specifically in Box 4.2. In this case we apply a forward selection model over 2000 Monte Carlo iterations. We find

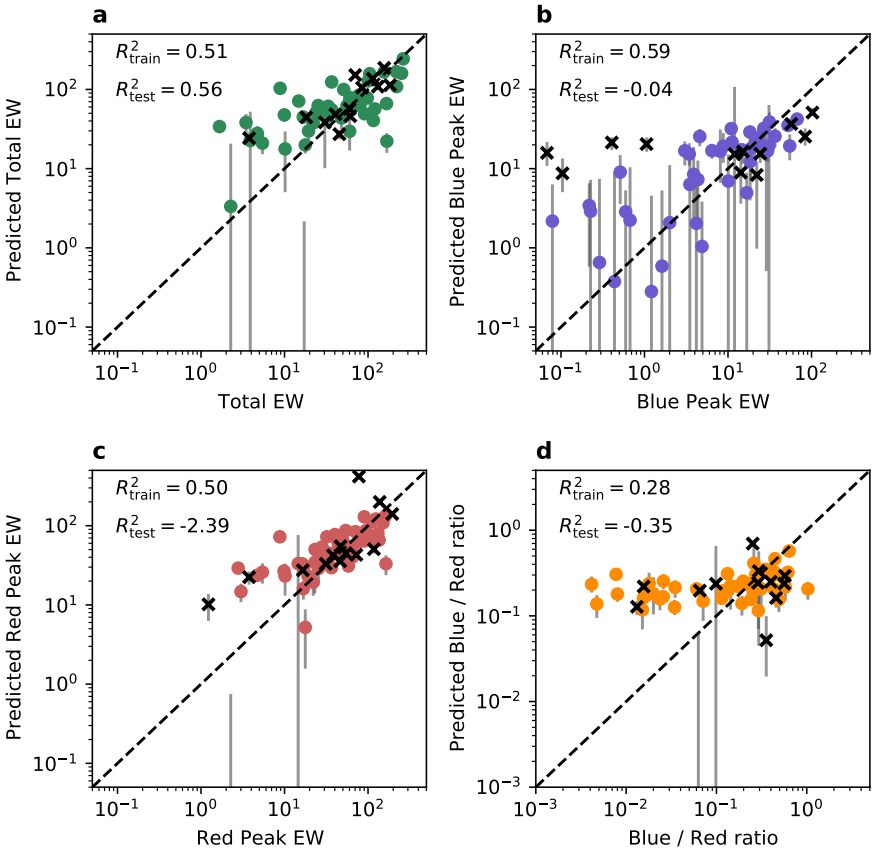

Figure 6.7: From **Paper V**. Panels show the predicted quantity on the y axis and the measured true quantity on x. Panel **a**: Total Lyα EW, Panel **b**: blue peak EW, Panel **c**: red peak EW, and Panel **d**: Blue over Red ratio. Colored points indicate the training sample and black crosses indicate test samples.

that for the luminosity the tracers of high and low ionization gas dominate, i.e. quantities such as [OIII] and [OII] luminosities, together with the flux of the bluest included Balmer line which in this case is Hβ. For the EW predictions the situation is less clear cut, but does seem to favor Hβ EW which traces the stellar evolution state, and the Hα/Hβ ratio which traces extinction by dust.

7. Conclusions and Outlook

A common thread throughout this thesis has been the complexity of understanding and interpreting Lyα emission and we have repeatedly shown relations between Lyα and other galaxy properties that are almost overwhelmed by scatter. The radiative transfer process of Lyα is quite simple from a physics point-of-view but it enables non-linear interactions between Lyα photons and many other components of the emitting galaxy. For instance, destruction of Lyα by dust is simple enough but when coupled with inhomogenous gas and dust distribution, complex gas kinematics, and ionization balances, the effect of a given amount of dust suddenly becomes much harder to judge, and will vary a lot.

However, despite all the difficulties Lyα is an extremely useful astrophysical tool that is now commonly used to detect high-redshift galaxies. The untapped potential of Lyα is also great and this is the underlying motivation for all the work in this thesis—if we can understand which physical processes dominate Lyα transfer and their effects we can potentially use Lyα to study many more things, such as star-formation in galaxies, Lyman continuum escape, and HI in the CGM and even in the IGM during the Epoch of Reionization.

Because of this, a substantial fraction of the work in this thesis has been devoted to Lyα correlations, both looking for new ones or quantifying their strength, such as in **Paper V**, or bringing multiple correlations together (**Paper I** and **Paper V**) to try to reduce the scatter and predict Lyα. We find that this approach works very well for luminosities, both total (**Paper I**) and divided into blue and red parts of the spectrum (**Paper V**) but that other Lyα quantities such as EW and $f_{esc}^{Ly\alpha}$ are harder to predict.

There are some interesting uses for relation of this type outside of the physical insights we may gain from finding the primary predictors. One example of such a use case is calculating the Lyα properties of large samples of simu-

lated galaxies from cosmological simulations. A full theoretical treatment of Lyα for these volumes is not possible since the spatial resolution is not even close to being sufficiently high. One intriguing possibility is then to use a predictive relation like the ones we developed and use it set the Lyα properties of galaxies in the simulation based on their ISM properties, thereby bypassing complex and expensive radiative transfer simulations. All of the physical properties our **Paper I** relation requires are known from simulations and therefore each galaxy can be assigned a Lyα luminosity and EW. This would enable for instance comparative studies of the simulated and observed Lyα luminosity functions from larger simulations than has previously been possible.

A further extension of this, that was mentioned briefly in the last chapter, is probabilistic inferences of the neutral fraction in the EoR. This type of analysis, such as that of Mason et al. (2018) for instance, relies on an assumed distribution of Lyα spectral shapes that escape from the ISM of galaxies. The simplest assumption is just a narrow spectral line at Lyα line center, but as we have shown many times in this thesis, this is not a particularly realistic assumption and most likely causes an overestimation of the intergalactic neutral fraction. Empirical relations for the spectral distribution of Lyα, such as those we attempted to derive in **Paper V**, can provide more realistic anchor points for such calculations. But from our results in **Paper V** it is clear that much work remains to be done in terms of predictive accuracy—especially for quantities such as the blue over red ratio. Saying that larger sample sizes are required to solve a problem is common in astronomy, and would most likely help here as well. However, in this case it is unlikely to make a big difference. Most likely what we need in this case is a broader data-set to work with, in the sense of more independent sources of information that complement the optical data, such high signal-to-noise measurements of UV absorption lines for individual galaxies for example.

If we want to expand samples and get more information to use in works like **Paper I** and **Paper V** we really need homogeneous analysis of Lyα spectra which has been hard to come by. Therefore we built a public database of Lyα spectra—the LASD which we presented in **Paper III**. The primary function of the LASD is perhaps not its database but the automated analysis pipeline which detects the redshift of Lyα lines and autonomously analyses and characterizes the emission line—measuring things like blue and peak fluxes, peak separa-

tions and line widths. This was the Lyα analysis we used in the predictions in **Paper V**.

Paper IV also took full advantage of the LASD samples and redshift determinations and used it to show the evolution of Lyα spectral profiles as a function of redshift and, perhaps most importantly, to show that when accounting for stochastic IGM absorption Lyα spectra are consistent with not changing across 10 billion years of cosmic history.

In **Paper II** we looked at the question of Lyα evolution across cosmic time, and in this case focusing specifically on the spatial distribution of Lyα emission. Wisotzki et al. (2016) noted a difference between their MUSE results and the early results of LARS (Hayes et al., 2014) with the LARS halos being smaller than those of high-z. To definitively answer whether this was true physical evolution or perhaps an artifact of the differing methodologies we presented a new sample of galaxies where a lot of care was taken to minimize systematics. We found that the Lyα halos in our new sample appear very similar to those at high-z. Taken together with **Paper IV** this suggests that the Lyα emission properties of highly star-forming galaxies appear relatively constant across cosmic time. This gives us confidence that the results we derive at low-z are actually applicable to galaxies in the first eras of galaxy formation.

In **Paper II** we also looked at the potential source of Lyα halo emission and found that it is most likely a combination of in-situ emission from recombination stemming from an extended stellar population and ionized gas halo and spatial scattering, based on deep UV continuum and Hα imaging. Testing whether there is a significant extended UV emission at high-z is complicated but stacking of current UV imaging could potentially provide evidence of the presence or absence of such a component. The recent launch of JWST opens up the possibility of observing the Hα of high redshift Lyα emitters directly, which will enable us to check whether our low-z results apply at high-z as well. However, cosmic surface brightness dimming is still a complication that needs to be taken into account.

Clearly, even with new instruments bringing unprecedented clarity to high redshift observations we still need low-redshift observations to understand the details of star-forming galaxies and Lyα escape and—hopefully—the work in this thesis has demonstrated some of what we can hope to understand.

Acknowledgements

I would like to thank my whole thesis group—Matt, Göran, and Claes, for their support during the long process of getting a PhD. In particular, many heartfelt thanks to Matt, without whose support, and enormous expertise, this could never have happened.

I also want to express my gratitude to the whole galaxy group and all its members, past and present, for creating such a positive and including workplace.

Finally, I want to thank my family for their support throughout this endeavor and especially Linn who not only put up with me for this whole ordeal and supported me during stressful times, but who was also the best office mate I can imagine during the two pandemic years.

List of Figures

References

Abel, T., Bryan, G. L., and Norman, M. L. (2002). The Formation of the First Star in the Universe. *Science*, 295:93–98. 21

Atek, H., Kunth, D., Schaerer, D., Hayes, M., Deharveng, J. M., Östlin, G., and Mas-Hesse, J. M. (2009). Empirical estimate of Ly α escape fraction in a statistical sample of Ly α emitters. *Astronomy & Astrophysics*, 506(2):L1–L4. 39

Bacon, R., Accardo, M., Adjali, L., Anwand, H., Bauer, S., Biswas, I., Blaizot, J., Boudon, D., Brau-Nogue, S., Brinchmann, J., Caillier, P., Capoani, L., Carollo, C. M., Contini, T., Couderc, P., Daguisé, E., Deiries, S., Delabre, B., Dreizler, S., Dubois, J., Dupieux, M., Dupuy, C., Emsellem, E., Fechner, T., Fleischmann, A., François, M., Gallou, G., Gharsa, T., Glindemann, A., Gojak, D., Guiderdoni, B., Hansali, G., Hahn, T., Jarno, A., Kelz, A., Koehler, C., Kosmalski, J., Laurent, F., Le Floch, M., Lilly, S. J., Lizon, J. L., Loupias, M., Manescau, A., Monstein, C., Nicklas, H., Olaya, J. C., Pares, L., Pasquini, L., Pécontal-Rousset, A., Pelló, R., Petit, C., Popow, E., Reiss, R., Remillieux, A., Renault, E., Roth, M., Rupprecht, G., Serre, D., Schaye, J., Soucail, G., Steinmetz, M., Streicher, O., Stuik, R., Valentin, H., Vernet, J., Weilbacher, P., Wisotzki, L., and Yerle, N. (2010). The MUSE second-generation VLT instrument. volume 7735 of *Society of Photo-Optical Instrumentation Engineers (SPIE) Conference Series*, page 773508. 51

Baker, J. G., Menzel, D. H., and Aller., L. H. (1938). Physical Processes in Gaseous Nebulae. V. Electron Temperatures. *The Astrophysical Journal*, 88:422. 28

Barnes, L. A., Garel, T., and Kacprzak, G. G. (2014). Ly-α and Mg II as Probes of Galaxies and Their Environment. *Publications of the Astronomical Society of the Pacific*, 126(945):969–1009. 29, 34

Bromm, V. (2013). Formation of the first stars. *Reports on Progress in Physics*, 76(11):112901. 21, 22

Bromm, V., Coppi, P. S., and Larson, R. B. (1999). Forming the First Stars in the Universe: The Fragmentation of Primordial Gas. *The Astrophysical Journal*, 527:L5–L8. 21

Bromm, V., Coppi, P. S., and Larson, R. B. (2002). The Formation of the First Stars. I. The Primordial Star-forming Cloud. *The Astrophysical Journal*, 564:23–51. 21

Calzetti, D. and Kinney, A. L. (1992). Lyman-alpha emission in star-forming galaxies - Low-redshift counterparts of primeval galaxies? *The Astrophysical Journal*, 399:L39. 38

Chen, Y., Steidel, C. C., Erb, D. K., Law, D. R., Trainor, R. F., Reddy, N. A., Shapley, A. E., Pahl, A. J., Strom, A. L., Lamb, N. R., Li, Z., and Rudie, G. C. (2021). The KBSS–KCWI survey: The connection between extended Ly α haloes and galaxy azimuthal angle at $z \sim 2$–3. *Monthly Notices of the Royal Astronomical Society*, 508(1):19–43. 58, 59, 61

Cullen, F., McLure, R. J., Dunlop, J. S., Carnall, A. C., McLeod, D. J., Shapley, A. E., Amorín, R., Bolzonella, M., Castellano, M., Cimatti, A., Cirasuolo, M., Cucciati, O., Fontana, A., Fontanot, F., Garilli, B., Guaita, L., Jarvis, M. J., Pentericci, L., Pozzetti, L., Talia, M., Zamorani, G., Calabrò, A., Cresci, G., Fynbo, J. P. U., Hathi, N. P., Giavalisco, M., Koekemoer, A., Mannucci, F., and Saxena, A. (2020). The VANDELS survey: A strong correlation between Ly α equivalent width and stellar metallicity at $3 \leq z \leq 5$. *Monthly Notices of the Royal Astronomical Society*, 495(1):1501–1510. 71

Diehl, S. and Statler, T. S. (2006). Adaptive binning of X-ray data with weighted Voronoi tessellations. *Monthly Notices of the Royal Astronomical Society*, 368(2):497–510. 56

Dijkstra, M. (2019). *Physics of Ly$$\alpha $$ Radiative Transfer*, volume 46 of *Saas-Fee Advanced Course*, pages 1–109. Springer Berlin Heidelberg, Berlin, Heidelberg. 25, 29, 30, 32, 33, 34, lxxxi

Dijkstra, M. and Loeb, A. (2009). Ly blobs as an observational signature of cold accretion streams into galaxies. *Monthly Notices of the Royal Astronomical Society*, 400(2):1109–1120. 29

Dopita, M. A. and Sutherland, R. S. (2003). *Astrophysics of the Diffuse Universe*. 29

Ellis, R. S., McLure, R. J., Dunlop, J. S., Robertson, B. E., Ono, Y., Schenker, M. A., Koekemoer, A., Bowler, R. A. A., Ouchi, M., Rogers, A. B., Curtis-Lake, E., Schneider, E., Charlot, S., Stark, D. P., Furlanetto, S. R., and Cirasuolo, M. (2013). The Abundance of Star-forming Galaxies in the Redshift Range 8.5-12: New Results from the 2012 Hubble Ultra Deep Field Campaign. *The Astrophysical Journal*, 763:L7. 23

Erb, D. K., Steidel, C. C., and Chen, Y. (2018). The Kinematics of Extended Ly α Emission in a Low-mass, Low-metallicity Galaxy at $z = 2.3$. *The Astrophysical Journal*, 862(1):L10. 58

Fan, X., Carilli, C., and Keating, B. (2006). Observational Constraints on Cosmic Reionization. *Annual Review of Astronomy and Astrophysics*, 44(1):415–462. 22

Fardal, M. A., Katz, N., Gardner, J. P., Hernquist, L., Weinberg, D. H., and Dave, R. (2001). Cooling Radiation and the Lyα Luminosity of Forming Galaxies. *The Astrophysical Journal*, 562(2):605–617. 29

Feldmeier, J. J., Hagen, A., Ciardullo, R., Gronwall, C., Gawiser, E., Guaita, L., Hagen, L. M. Z., Bond, N. A., Acquaviva, V., Blanc, G. A., Orsi, A., and Kurczynski, P. (2013). SEARCHING FOR NEUTRAL HYDROGEN HALOS AROUND $z \sim 2.1$ AND $z \sim 3.1$ Lyα EMITTING GALAXIES. *The Astrophysical Journal*, 776(2):75. 49

Ferland, G. J. (1999). Hydrogen Emission from Low Column Density Gas: Case C. *Publications of the Astronomical Society of the Pacific*, 111(766):1524–1528. 28

Flury, S. R., Jaskot, A. E., Ferguson, H. C., Worseck, G., Makan, K., Chisholm, J., Saldana-Lopez, A., Schaerer, D., McCandless, S., Wang, B., Ford, N. M., Heckman, T., Ji, Z., Giavalisco, M., Amorin, R., Atek, H., Blaizot, J., Borthakur, S., Carr, C., Castellano, M., Cristiani, S., de Barros, S., Dickinson, M., Finkelstein, S. L., Fleming, B., Fontanot, F., Garel, T., Grazian, A., Hayes, M., Henry, A., Mauerhofer, V., Micheva, G., Oey, M. S., Ostlin, G., Papovich, C., Pentericci, L., Ravindranath, S., Rosdahl, J., Rutkowski, M., Santini, P., Scarlata, C., Teplitz, H., Thuan, T., Trebitsch, M., Vanzella, E., Verhamme, A., and Xu, X. (2022a). The Low-Redshift Lyman Continuum Survey I: New, Diverse Local Lyman-Continuum Emitters. *arXiv:2201.11716 [astro-ph]*. 41

Flury, S. R., Jaskot, A. E., Ferguson, H. C., Worseck, G., Makan, K., Chisholm, J., Saldana-Lopez, A., Schaerer, D., McCandliss, S., Wang, B., Ford, N. M., Oey, M. S., Heckman, T., Ji, Z., Giavalisco, M., Amorin, R., Atek, H., Blaizot, J., Borthakur, S., Carr, C., Castellano, M., Cristiani, S., de Barros, S., Dickinson, M., Finkelstein, S. L., Fleming, B., Fontanot, F., Garel, T., Grazian, A., Hayes, M., Henry, A., Mauerhofer, V., Micheva, G., Ostlin, G., Papovich, C., Pentericci, L., Ravindranath, S., Rosdahl, J., Rutkowski, M., Santini, P., Scarlata, C., Teplitz, H., Thuan, T., Trebitsch, M., Vanzella, E., Verhamme, A., and Xu, X. (2022b). The Low-Redshift Lyman Continuum Survey II: New Insights into LyC Diagnostics. *arXiv:2203.15649 [astro-ph]*. 41

Giavalisco, M., Koratkar, A., and Calzetti, D. (1996). Obscuration of LY alpha Photons in Star-forming Galaxies. *The Astrophysical Journal*, 466:831. 38, 39, lxxxi

Goerdt, T., Dekel, A., Sternberg, A., Ceverino, D., Teyssier, R., and Primack, J. R. (2010). Gravity-driven Lyα blobs from cold streams into galaxies: Cold streams as Lyα blobs. *Monthly Notices of the Royal Astronomical Society*, 407(1):613–631. 29

Greif, T. H. (2015). The numerical frontier of the high-redshift Universe. *Computational Astrophysics and Cosmology*, 2(1):3. 21

Gronke, M. (2017). Modeling 237 Lyman- α spectra of the MUSE-Wide survey. *Astronomy & Astrophysics*, 608:A139. 63

Gronke, M., Bull, P., and Dijkstra, M. (2015). A SYSTEMATIC STUDY OF Ly α TRANSFER THROUGH OUTFLOWING SHELLS: MODEL PARAMETER ESTIMATION. *The Astrophysical Journal*, 812(2):123. 63, 64

Hartmann, L. W., Huchra, J. P., and Geller, M. J. (1984). How to find galaxies at high redshift. *The Astrophysical Journal*, 287:487. 39

Hartmann, L. W., Huchra, J. P., Geller, M. J., O'Brien, P., and Wilson, R. (1988). Lyman-alpha emission in star-forming galaxies. *The Astrophysical Journal*, 326:101. 37, 38, 39

Hayes, M. (2019). *Lyman Alpha Emission and Absorption in Local Galaxies*, volume 46 of *Saas-Fee Advanced Course*, pages 319–398. Springer Berlin Heidelberg, Berlin, Heidelberg. 40, 52, 53

Hayes, M., Östlin, G., Duval, F., Sandberg, A., Guaita, L., Melinder, J., Adamo, A., Schaerer, D., Verhamme, A., Orlitová, I., Mas-Hesse, J. M., Cannon, J. M., Atek, H., Kunth, D., Laursen, P., Otí-Floranes, H., Pardy, S., Rivera-Thorsen, T., and Herenz, E. C. (2014). THE LYMAN ALPHA REFERENCE SAMPLE. II. *HUBBLE SPACE TELESCOPE* IMAGING RESULTS, INTEGRATED PROPERTIES, AND TRENDS. *The Astrophysical Journal*, 782(1):6. 41, 54, 56, 77

Hayes, M., Östlin, G., Mas-Hesse, J. M., and Kunth, D. (2009). CONTINUUM SUBTRACTING LYMAN-ALPHA IMAGES: LOW-REDSHIFT STUDIES USING THE SOLAR BLIND CHANNEL OF *HST* /ACS. *The Astronomical Journal*, 138(3):911–922. 52, 56

Heckman, T. M., Borthakur, S., Overzier, R., Kauffmann, G., Basu-Zych, A., Leitherer, C., Sembach, K., Martin, D. C., Rich, R. M., Schiminovich, D., and Seibert, M. (2011). EXTREME FEEDBACK AND THE EPOCH OF REIONIZATION: CLUES IN THE LOCAL UNIVERSE. *The Astrophysical Journal*, 730(1):5. 46, 62

Henry, A., Scarlata, C., Martin, C. L., and Erb, D. (2015). Ly α EMISSION FROM GREEN PEAS: THE ROLE OF CIRCUMGALACTIC GAS DENSITY, COVERING, AND KINEMATICS. *The Astrophysical Journal*, 809(1):19. 29, 40

Hu, E. M., Cowie, L. L., Capak, P., McMahon, R. G., Hayashino, T., and Komiyama, Y. (2004). The Luminosity Function of Ly Emitters at Redshift z ~5.7. *The Astronomical Journal*, 127(2):563–575. 48

Hu, E. M. and McMahon, R. G. (1996). Detection of Lyman-α-emitting galaxies at redshift 4.55. *Nature*, 382(6588):231–233. 48

Ilbert, O., Arnouts, S., Le Floc'h, E., Aussel, H., Bethermin, M., Capak, P., Hsieh, B.-C., Kajisawa, M., Karim, A., Le Fèvre, O., Lee, N., Lilly, S., McCracken, H. J., Michel-Dansac, L., Moutard, T., Renzini, M. A., Salvato, M., Sanders, D. B., Scoville, N., Sheth, K., Silverman, J. D., Smolčić, V., Taniguchi, Y., and Tresse, L. (2015). Evolution of the specific star formation rate function at $z < 1.4$ Dissecting the mass-SFR plane in COSMOS and GOODS. *Astronomy & Astrophysics*, 579:A2. 24

Inoue, A. K., Shimizu, I., Iwata, I., and Tanaka, M. (2014). An updated analytic model for attenuation by the intergalactic medium. *Monthly Notices of the Royal Astronomical Society*, 442(2):1805–1820. 67

Izotov, Y. I., Orlitová, I., Schaerer, D., Thuan, T. X., Verhamme, A., Guseva, N. G., and Worseck, G. (2016). Eight per cent leakage of Lyman continuum photons from a compact, star-forming dwarf galaxy. *Nature*, 529(7585):178–180. 41

Izotov, Y. I., Schaerer, D., Worseck, G., Verhamme, A., Guseva, N. G., Thuan, T. X., Orlitová, I., and Fricke, K. J. (2020). Diverse properties of Ly α emission in low-redshift compact star-forming galaxies with extremely high [O iii]/[O ii] ratios. *Monthly Notices of the Royal Astronomical Society*, 491(1):468–482. 41

Izotov, Y. I., Worseck, G., Schaerer, D., Guseva, N. G., Chisholm, J., Thuan, T. X., Fricke, K. J., and Verhamme, A. (2021). Lyman continuum leakage from low-mass galaxies with $M \star$ < 108 M$\odot$. *Monthly Notices of the Royal Astronomical Society*, 503(2):1734–1752. 41

Izotov, Y. I., Worseck, G., Schaerer, D., Guseva, N. G., Thuan, T. X., Fricke, Verhamme, A., and Orlitová, I. (2018). Low-redshift Lyman continuum leaking galaxies with high [O iii]/[O ii] ratios. *Monthly Notices of the Royal Astronomical Society*, 478(4):4851–4865. 41

Jaskot, A. E. and Oey, M. S. (2013). THE ORIGIN AND OPTICAL DEPTH OF IONIZING RADIATION IN THE "GREEN PEA" GALAXIES. *The Astrophysical Journal*, 766(2):91. 41

Kalberla, P. M. and Kerp, J. (2009). The H I Distribution of the Milky Way. *Annual Review of Astronomy and Astrophysics*, 47(1):27–61. 30

Kunth, D., Mas-Hesse, J. M., Terlevich, E., Terlevich, R., Lequeux, J., and Fall, S. M. (1998). HST study of Lyman-alpha emission in star-forming galaxies: The effect of neutral gas flows. *Astronomy & Astrophysics*, 334:11–20. 40

Leclercq, F., Bacon, R., Verhamme, A., Garel, T., Blaizot, J., Brinchmann, J., Cantalupo, S., Claeyssens, A., Conseil, S., Contini, T., Hashimoto, T., Herenz, E. C., Kusakabe, H., Marino, R. A., Maseda, M., Matthee, J., Mitchell, P., Pezzulli, G., Richard, J., Schmidt, K. B., and Wisotzki, L. (2020). The MUSE *Hubble* Ultra Deep Field Survey: XIII. Spatially resolved spectral properties of Lyman α haloes around star-forming galaxies at $z > 3$. *Astronomy & Astrophysics*, 635:A82. 58, 59, 61

Leclercq, F., Bacon, R., Wisotzki, L., Mitchell, P., Garel, T., Verhamme, A., Blaizot, J., Hashimoto, T., Herenz, E. C., Conseil, S., Cantalupo, S., Inami, H., Contini, T., Richard, J., Maseda, M., Schaye, J., Marino, R. A., Akhlaghi, M., Brinchmann, J., and Carollo, M. (2017). The MUSE *Hubble* Ultra Deep Field Survey: VIII. Extended Lyman- α haloes around high- z star-forming galaxies. *Astronomy & Astrophysics*, 608:A8. 51, 56, 58

Leitherer, C., Schaerer, D., Goldader, J. D., Delgado, R. M. G., Robert, C., Kune, D. F., de Mello, D. F., Devost, D., and Heckman, T. M. (1999). Starburst99: Synthesis Models for Galaxies with Active Star Formation. *The Astrophysical Journal Supplement Series*, 123(1):3–40. 40, 71

Leslie, S. K., Schinnerer, E., Liu, D., Magnelli, B., Algera, H., Karim, A., Davidzon, I., Gozaliasl, G., Jiménez-Andrade, E. F., Lang, P., Sargent, M. T., Novak, M., Groves, B., Smolčić, V., Zamorani, G., Vaccari, M., Battisti, A., Vardoulaki, E., Peng, Y., and Kartaltepe, J. (2020). The VLA-COSMOS 3 GHz Large Project: Evolution of Specific Star Formation Rates out to $z \sim 5$. *The Astrophysical Journal*, 899(1):58. 24

Lujan Niemeyer, M., Komatsu, E., Byrohl, C., Davis, D., Fabricius, M., Gebhardt, K., Hill, G. J., Wisotzki, L., Bowman, W. P., Ciardullo, R., Farrow, D. J., Finkelstein, S. L., Gawiser, E., Gronwall, C., Jeong, D., Landriau, M., Liu, C., Cooper, E. M., Ouchi, M., Schneider, D. P., and Zeimann, G. R. (2022). Surface Brightness Profile of Lyman-α Halos out to 320 kpc in HETDEX. *The Astrophysical Journal*, 929(1):90. 25

Luridiana, V., Simón-Díaz, S., Cerviño, M., Delgado, R. M. G., Porter, R. L., and Ferland, G. J. (2009). FLUORESCENT EXCITATION OF BALMER LINES IN GASEOUS NEBULAE: Case D. *The Astrophysical Journal*, 691(2):1712–1728. 28

Madau, P. and Dickinson, M. (2014). Cosmic Star-Formation History. *Annual Review of Astronomy and Astrophysics*, 52(1):415–486. 14, 23, lxxxi

Mallery, R. P., Mobasher, B., Capak, P., Kakazu, Y., Masters, D., Ilbert, O., Hemmati, S., Scarlata, C., Salvato, M., McCracken, H., LeFevre, O., and Scoville, N. (2012). Lyα EMISSION FROM HIGH-REDSHIFT SOURCES IN COSMOS. *The Astrophysical Journal*, 760(2):128. 39, 40

Mason, C. A., Treu, T., Dijkstra, M., Mesinger, A., Trenti, M., Pentericci, L., de Barros, S., and Vanzella, E. (2018). The Universe Is Reionizing at $z \sim 7$: Bayesian Inference of the IGM Neutral Fraction Using Ly α Emission from Galaxies. *The Astrophysical Journal*, 856(1):2. 69, 76

Matsuda, Y., Yamada, T., Hayashino, T., Yamauchi, R., Nakamura, Y., Morimoto, N., Ouchi, M., Ono, Y., Umemura, M., and Mori, M. (2012). Diffuse Lyα haloes around Lyα emitters at z=3: Do dark matter distributions determine the Lyα spatial extents?: Lyα haloes at z = 3. *Monthly Notices of the Royal Astronomical Society*, 425(2):878–883. 49

McGreer, I. D., Mesinger, A., and D'Odorico, V. (2015). Model-independent evidence in favour of an end to reionization by z $\approx$ 6. *Monthly Notices of the Royal Astronomical Society*, 447(1):499–505. 22

Meier, D. L. and Terlevich, R. (1981). Extragalactic H II regions in the UV - Implications for primeval galaxies. *The Astrophysical Journal*, 246:L109. 37, 39

Mellema, G., Koopmans, L. V. E., Abdalla, F. A., Bernardi, G., Ciardi, B., Daiboo, S., de Bruyn, A. G., Datta, K. K., Falcke, H., Ferrara, A., Iliev, I. T., Iocco, F., Jelić, V., Jensen, H., Joseph, R., Labroupoulos, P., Meiksin, A., Mesinger, A., Offringa, A. R., Pandey, V. N., Pritchard, J. R., Santos, M. G., Schwarz, D. J., Semelin, B., Vedantham, H., Yatawatta, S., and Zaroubi, S. (2013). Reionization and the Cosmic Dawn with the Square Kilometre Array. *Experimental Astronomy*, 36(1-2):235–318. 22

Momose, R., Ouchi, M., Nakajima, K., Ono, Y., Shibuya, T., Shimasaku, K., Yuma, S., Mori, M., and Umemura, M. (2014). Diffuse Lyα haloes around galaxies at z = 2.2–6.6: Implications for galaxy formation and cosmic reionization. *Monthly Notices of the Royal Astronomical Society*, 442(1):110–120. 50

Morrissey, P., Matuszewski, M., Martin, D. C., Neill, J. D., Epps, H., Fucik, J., Weber, B., Darvish, B., Adkins, S., Allen, S., Bartos, R., Belicki, J., Cabak, J., Callahan, S., Cowley, D., Crabill, M., Deich, W., Delecroix, A., Doppman, G., Hilyard, D., James, E., Kaye, S., Kokorowski, M., Kwok, S., Lanclos, K., Milner, S., Moore, A., O'Sullivan, D., Parihar, P., Park, S., Phillips, A., Rizzi, L., Rockosi, C., Rodriguez, H., Salaun, Y., Seaman, K., Sheikh, D., Weiss, J., and Zarzaca, R. (2018). The Keck Cosmic Web Imager Integral Field Spectrograph. *The Astrophysical Journal*, 864(1):93. 51

Murphy, L. J., Groh, J. H., Farrell, E., Meynet, G., Ekström, S., Tsiatsiou, S., Hackett, A., and Martinet, S. (2021). Ionizing photon production of Population III stars: Effects of rotation, convection, and initial mass function. *Monthly Notices of the Royal Astronomical Society*, 506(4):5731–5749. 21

Naidu, R. P., Matthee, J., Oesch, P. A., Conroy, C., Sobral, D., Pezzulli, G., Hayes, M., Erb, D., Amorín, R., Gronke, M., Schaerer, D., Tacchella, S., Kerutt, J., Paulino-Afonso, A., Calhau, J., Llerena, M., and Röttgering, H. (2022). The synchrony of production and escape: Half the bright Lyα emitters at $z \approx 2$ have Lyman continuum escape fractions $\approx$50. *Monthly Notices of the Royal Astronomical Society*, 510(3):4582–4607. 62

Östlin, G., Hayes, M., Duval, F., Sandberg, A., Rivera-Thorsen, T., Marquart, T., Orlitová, I., Adamo, A., Melinder, J., Guaita, L., Atek, H., Cannon, J. M., Gruyters, P., Herenz, E. C., Kunth, D., Laursen, P., Mas-Hesse, J. M., Micheva, G., Otí-Floranes, H., Pardy, S. A., Roth, M. M., Schaerer, D., and Verhamme, A. (2014). THE Lyα REFERENCE SAMPLE. I. SURVEY OUTLINE AND FIRST RESULTS FOR MARKARIAN 259. *The Astrophysical Journal*, 797(1):11. 52, 53, 56

Ouchi, M., Harikane, Y., Shibuya, T., Shimasaku, K., Taniguchi, Y., Konno, A., Kobayashi, M., Kajisawa, M., Nagao, T., Ono, Y., Inoue, A. K., Umemura, M., Mori, M., Hasegawa, K., Higuchi, R., Komiyama, Y., Matsuda, Y., Nakajima, K., Saito, T., and Wang, S.-Y. (2018). Systematic Identification of LAEs for Visible Exploration and Reionization Research Using Subaru HSC (SILVERRUSH). I. Program strategy and clustering properties of $\sim$2000 Lyα emitters at z = 6–7 over the 0.3–0.5 Gpc2 survey area†. *Publications of the Astronomical Society of Japan*, 70(SP1). 25

Partridge, R. B. and Peebles, P. J. E. (1967). Are Young Galaxies Visible? *The Astrophysical Journal*, 147:868. 25, 37

Planck Collaboration, Ade, P. A. R., Aghanim, N., Arnaud, M., Ashdown, M., Aumont, J., Baccigalupi, C., Banday, A. J., Barreiro, R. B., Bartlett, J. G., Bartolo, N., Battaner, E., Battye, R., Benabed, K., Benoît, A., Benoit-Lévy, A., Bernard, J.-P., Bersanelli, M., Bielewicz, P., Bock, J. J., Bonaldi, A., Bonavera, L., Bond, J. R., Borrill, J., Bouchet, F. R., Boulanger, F., Bucher, M., Burigana, C., Butler, R. C., Calabrese, E., Cardoso, J.-F., Catalano, A., Challinor, A., Chamballu, A., Chary, R.-R., Chiang, H. C., Chluba, J., Christensen, P. R., Church, S., Clements, D. L., Colombi, S., Colombo, L. P. L., Combet, C., Coulais, A., Crill, B. P., Curto, A., Cuttaia, F., Danese, L., Davies, R. D., Davis, R. J., de Bernardis, P., de Rosa, A., de Zotti, G., Delabrouille, J., Désert, F.-X., Di Valentino, E., Dickinson, C., Diego, J. M., Dolag, K., Dole, H., Donzelli, S., Doré, O., Douspis, M., Ducout, A., Dunkley, J., Dupac, X., Efstathiou, G., Elsner, F., Enßlin, T. A., Eriksen, H. K., Farhang, M., Fergusson, J., Finelli, F., Forni, O., Frailis, M., Fraisse, A. A., Franceschi, E., Frejsel, A., Galeotta, S., Galli, S., Ganga, K., Gauthier, C., Gerbino, M., Ghosh, T., Giard, M., Giraud-Héraud, Y., Giusarma, E., Gjerløw, E., González-Nuevo, J., Górski, K. M., Gratton, S., Gregorio, A., Gruppuso, A., Gudmundsson, J. E., Hamann, J., Hansen, F. K., Hanson, D., Harrison, D. L., Helou, G., Henrot-Versillé, S., Hernández-Monteagudo, C., Herranz, D., Hildebrandt, S. R., Hivon, E., Hobson, M., Holmes, W. A., Hornstrup, A., Hovest, W., Huang, Z., Huffenberger, K. M., Hurier, G., Jaffe, A. H., Jaffe, T. R., Jones, W. C., Juvela, M., Keihänen, E., Keskitalo, R., Kisner, T. S., Kneissl, R., Knoche, J., Knox, L., Kunz, M., Kurki-Suonio, H., Lagache, G., Lähteenmäki, A., Lamarre, J.-M., Lasenby, A., Lattanzi, M., Lawrence, C. R., Leahy, J. P., Leonardi, R., Lesgourgues, J.,

Levrier, F., Lewis, A., Liguori, M., Lilje, P. B., Linden-Vørnle, M., López-Caniego, M., Lubin, P. M., Macías-Pérez, J. F., Maggio, G., Maino, D., Mandolesi, N., Mangilli, A., Marchini, A., Maris, M., Martin, P. G., Martinelli, M., Martínez-González, E., Masi, S., Matarrese, S., McGehee, P., Meinhold, P. R., Melchiorri, A., Melin, J.-B., Mendes, L., Mennella, A., Migliaccio, M., Millea, M., Mitra, S., Miville-Deschênes, M.-A., Moneti, A., Montier, L., Morgante, G., Mortlock, D., Moss, A., Munshi, D., Murphy, J. A., Naselsky, P., Nati, F., Natoli, P., Netterfield, C. B., Nørgaard-Nielsen, H. U., Noviello, F., Novikov, D., Novikov, I., Oxborrow, C. A., Paci, F., Pagano, L., Pajot, F., Paladini, R., Paoletti, D., Partridge, B., Pasian, F., Patanchon, G., Pearson, T. J., Perdereau, O., Perotto, L., Perrotta, F., Pettorino, V., Piacentini, F., Piat, M., Pierpaoli, E., Pietrobon, D., Plaszczynski, S., Pointecouteau, E., Polenta, G., Popa, L., Pratt, G. W., Prézeau, G., Prunet, S., Puget, J.-L., Rachen, J. P., Reach, W. T., Rebolo, R., Reinecke, M., Remazeilles, M., Renault, C., Renzi, A., Ristorcelli, I., Rocha, G., Rosset, C., Rossetti, M., Roudier, G., Rouillé d'Orfeuil, B., Rowan-Robinson, M., Rubiño-Martín, J. A., Rusholme, B., Said, N., Salvatelli, V., Salvati, L., Sandri, M., Santos, D., Savelainen, M., Savini, G., Scott, D., Seiffert, M. D., Serra, P., Shellard, E. P. S., Spencer, L. D., Spinelli, M., Stolyarov, V., Stompor, R., Sudiwala, R., Sunyaev, R., Sutton, D., Suur-Uski, A.-S., Sygnet, J.-F., Tauber, J. A., Terenzi, L., Toffolatti, L., Tomasi, M., Tristram, M., Trombetti, T., Tucci, M., Tuovinen, J., Türler, M., Umana, G., Valenziano, L., Valiviita, J., Van Tent, F., Vielva, P., Villa, F., Wade, L. A., Wandelt, B. D., Wehus, I. K., White, M., White, S. D. M., Wilkinson, A., Yvon, D., Zacchei, A., and Zonca, A. (2016). *Planck* 2015 results: XIII. Cosmological parameters. *Astronomy & Astrophysics*, 594:A13. 22

Rasekh, A., Melinder, J., Östlin, G., Hayes, M., Herenz, E. C., Runnholm, A., Kunth, D., Hesse, J. M. M., Verhamme, A., and Cannon, J. M. (2021). The Lyman Alpha Reference Sample XII: Morphology of extended Lyman alpha emission in star-forming galaxies. *arXiv:2110.01626 [astro-ph]*. 54

Rivera-Thorsen, T. E., Dahle, H., Chisholm, J., Florian, M. K., Gronke, M., Rigby, J. R., Gladders, M. D., Mahler, G., Sharon, K., and Bayliss, M. (2019). Gravitational lensing reveals ionizing ultraviolet photons escaping from a distant galaxy. *Science*, 366(6466):738–741. 62

Rivera-Thorsen, T. E., Hayes, M., Östlin, G., Duval, F., Orlitová, I., Verhamme, A., Mas-Hesse, J. M., Schaerer, D., Cannon, J. M., Otí-Floranes, H., Sandberg, A., Guaita, L., Adamo, A., Atek, H., Herenz, E. C., Kunth, D., Laursen, P., and Melinder, J. (2015). THE LYMAN ALPHA REFERENCE SAMPLE. V. THE IMPACT OF NEUTRAL ISM KINEMATICS AND GEOMETRY ON Ly α ESCAPE. *The Astrophysical Journal*, 805(1):14. 40, 41

Runnholm, A., Hayes, M., Melinder, J., Rivera-Thorsen, E., Östlin, G., Cannon, J., and Kunth, D. (2020). The Lyman Alpha Reference Sample. X. Predicting Ly α Output from Star-forming Galaxies Using Multivariate Regression. *The Astrophysical Journal*, 892(1):48. 43

Scarlata, C., Colbert, J., Teplitz, H. I., Panagia, N., Hayes, M., Siana, B., Rau, A., Francis, P., Caon, A., Pizzella, A., and Bridge, C. (2009). THE EFFECT OF DUST GEOMETRY ON THE Lyα OUTPUT OF GALAXIES. *The Astrophysical Journal*, 704(2):L98–L102. 39

Schreiber, C., Pannella, M., Elbaz, D., Béthermin, M., Inami, H., Dickinson, M., Magnelli, B., Wang, T., Aussel, H., Daddi, E., Juneau, S., Shu, X., Sargent, M. T., Buat, V., Faber, S. M., Ferguson, H. C., Giavalisco, M., Koekemoer, A. M., Magdis, G., Morrison, G. E., Papovich, C., Santini, P., and Scott, D. (2015). The *Herschel* view of the dominant mode of galaxy growth from $z = 4$ to the present day. *Astronomy & Astrophysics*, 575:A74. 23, 24, lxxxi

Steidel, C. C., Bogosavljević, M., Shapley, A. E., Kollmeier, J. A., Reddy, N. A., Erb, D. K., and Pettini, M. (2011). DIFFUSE Lyα EMITTING HALOS: A GENERIC PROPERTY OF HIGH-REDSHIFT STAR-FORMING GALAXIES. *The Astrophysical Journal*, 736(2):160. 49, 50, 51, lxxxi

Terlevich, E., Díaz, A. I., Terlevich, R., and Vargas, M. L. G. (1993). New detections of Ly α emission in young galaxies. *Monthly Notices of the Royal Astronomical Society*, 260(1):3–8. 39

Thuan, T. X., Izotov, Y. I., and Lipovetsky, V. A. (1997). *Hubble Space Telescope* Observations of the Blue Compact Dwarf SBS 0335-052: A Probable Young Galaxy. *The Astrophysical Journal*, 477(2):661–672. 40

Tolman, R. C. (1930). ON THE ESTIMATION OF DISTANCES IN A CURVED UNIVERSE WITH A NON-STATIC LINE ELEMENT. *Proceedings of the National Academy of Sciences*, 16(7):511–520. 49

Tolman, R. C. (1934). Effect of Inhomogeneity on Cosmological Models. *Proceedings of the National Academy of Sciences*, 20(3):169–176. 49

Trainor, R. F., Strom, A. L., Steidel, C. C., Rudie, G. C., Chen, Y., and Theios, R. L. (2019). Predicting Lyα Emission from Galaxies via Empirical Markers of Production and Escape in the KBSS. *arXiv:1908.04794 [astro-ph]*. 42, 43, 45, lxxxi

Urrutia, T., Wisotzki, L., Kerutt, J., Schmidt, K. B., Herenz, E. C., Klar, J., Saust, R., Werhahn, M., Diener, C., Caruana, J., Krajnović, D., Bacon, R., Boogaard, L., Brinchmann, J., Enke, H., Maseda, M., Nanayakkara, T., Richard, J., Steinmetz, M., and Weilbacher, P. M. (2019). The MUSE-Wide Survey: Survey description and first data release. *Astronomy & Astrophysics*, 624:A141. 25

Verhamme, A., Garel, T., Ventou, E., Contini, T., Bouché, N., Herenz, E., Richard, J., Bacon, R., Schmidt, K., Maseda, M., Marino, R., Brinchmann, J., Cantalupo, S., Caruana, J., Clément, B., Diener, C., Drake, A., Hashimoto, T., Inami, H., Kerutt, J., Kollatschny, W., Leclercq, F., Patrício, V., Schaye, J., Wisotzki, L., and Zabl, J. (2018). Recovering the systemic redshift of galaxies from their Lyman alpha line profile. *Monthly Notices of the Royal Astronomical Society: Letters*, 478(1):L60–L65. 65

Verhamme, A., Schaerer, D., Atek, H., and Tapken, C. (2008). 3D Ly α radiation transfer: III. Constraints on gas and stellar properties of $z \sim 3$ Lyman break galaxies (LBG) and implications for high- z LBGs and Ly α emitters. *Astronomy & Astrophysics*, 491(1):89–111. 63

Wisotzki, L., Bacon, R., Blaizot, J., Brinchmann, J., Herenz, E. C., Schaye, J., Bouché, N., Cantalupo, S., Contini, T., Carollo, C. M., Caruana, J., Courbot, J.-B., Emsellem, E., Kamann, S., Kerutt, J., Leclercq, F., Lilly, S. J., Patrício, V., Sandin, C., Steinmetz, M., Straka, L. A., Urrutia, T., Verhamme, A., Weilbacher, P. M., and Wendt, M. (2016). Extended Lyman α haloes around individual high-redshift galaxies revealed by MUSE. *Astronomy & Astrophysics*, 587:A98. 51, 77

Wu, C.-C., Boggess, A., and Gull, T. R. (1983). Prominent ultraviolet emission lines from Type 1 Seyfert galaxies. *The Astrophysical Journal*, 266:28. 37, 38

Yang, H., Malhotra, S., Gronke, M., Rhoads, J. E., Leitherer, C., Wofford, A., Jiang, T., Dijkstra, M., Tilvi, V., and Wang, J. (2017). Ly α Profile, Dust, and Prediction of Ly α Escape Fraction in Green Pea Galaxies. *The Astrophysical Journal*, 844(2):171. 42, 43, 44, 45, lxxxi